ELSEVIER

Coordination Chemistry Reviews
193–195 (1999) 769–835

COORDINATION CHEMISTRY REVIEWS

www.elsevier.com/locate/ccr

Coordination chemistry of oxazoline ligands

Montserrat Gómez, Guillermo Muller *, Mercè Rocamora

Departament de Química Inorgànica, Universitat de Barcelona, Martí i Franquès, 1-11, E-08028 Barcelona, Spain

Received 30 October 1998; received in revised form 16 February 1999; accepted 13 March 1999

Contents

Abstract

4,5-Dihydro-1,3-oxazole ligands (commonly known as 2-oxazolines or simply oxazolines) have been used by many research groups as chiral auxiliaries in transition metal-catalyzed asymmetric organic syntheses. The oxazolines show a number of attractive characteristics:

* Corresponding author. Tel.: +34-93-4021273; fax: +34-93-4907725.
E-mail address: gm@kripto.qui.ub.es (G. Muller)

PII: S0010-8545(99)00086-7

versatility of ligand design, straightforward synthesis of ligands from readily available precursors, and modulation of the chiral centers, which are located near the donor atoms. This review focuses on the transition metal coordination chemistry of oxazolines. It surveys data describing structural characterization in both solid state (X-ray diffraction) and solution (NMR spectroscopy).

Keywords: Oxazoline; Transition metal; Coordination compounds; X-ray; NMR

1. Introduction

In recent years, the activity of new *N*-donor ligands in several catalytic reactions, in which previously only P-donor ligands had been used (for example, allylic substitutions, Heck reactions, hydrosilylations, cyclopropanations and Diels–Alder additions), has been demonstrated [1]. Of these, chiral *N*-donor ligands have been used successfully in the asymmetric version of the catalytic reactions. Oxazolines and their related molecules are among the most frequently studied chiral nitrogen-containing ligands due to the high enantioselectivities achieved in a range of processes. While the applications of this type of ligands have recently been reviewed [2,3], no report on the coordination chemistry of such ligands has been published to date.

The oxazoline ligands used in asymmetric synthesis are generally polydentate ligands containing one or more oxazoline fragments. The chelation effect is related to the constrictions imposed by the coordination to the metal complex, so that only one stereogenic center lies near the coordination sphere. This favors strong asymmetric induction in the catalytic reaction. The arrangement also allows the modulation of ligand substituents, depending on the specific asymmetric process, thereby improving its enantioselectivity. The modification of the chelate ring size is another means of optimizing the inductive effect at the metal center. Furthermore, combinations of soft and hard donor groups are used in designing highly active bidentate ligands. This furnishes their directing capacity with an electronic factor [4].

As the number of catalytic applications of oxazolines to organic processes has increased, the mechanism of these reactions and the characterization of precursors and intermediate metal species have also been studied. Recent developments in instrumental techniques, both for solid state and solution samples, have permitted the structures of the metal complexes to be determined.

The versatility of the oxazoline ligands prompted us to prepare this report, in which we survey the coordination chemistry of the ligands emphasizing the structural characteristics of the transition metal complexes.

2. Oxazoline ligands: structural aspects

Although the oxazoline cycle was first prepared in 1884 [5], it is only in the last

two decades that the ligands containing oxazoline groups have been extensively applied, principally in asymmetric catalytic processes. Despite this, oxazolines have been used widely in many areas of chemistry (reviewed in 1949 and 1971 [6]), given the versatility of this ring which acts as a protector group, coordinating ligand, and activation moiety. Furthermore, the oxazoline ligating group occurs naturally in certain classes of microbial iron chelators [7].

The widespread use of such ligands in a great variety of organic transformations is due basically to the ease with which they can be prepared from natural available aminoacids and synthetic aminoalcohols, and the stability of the oxazoline ring. While oxazoline moiety is sensitive to mineral and Lewis acids, it is resistant to nucleophiles, bases, radicals, and even a number of acids, if no other labile functional groups are present on the substrate [8]. Moreover, in the case of chiral oxazolines, their stereocenter lies very near the metal sphere in the catalytic species, upon chelate *N*-coordination of the ligand to the metal atom.

Usually, oxazoline ligands are synthesized from aminoalcohols (easily prepared by reduction of α-aminoacids) and nitrile or carboxylic acid derivatives [9] (Scheme 1), although other procedures are also used because of the particularly sensitive functionalities present on the precursors [10].

In order to analyze the structural features of these ligands, a Cambridge Structural search has been undertaken [11]. Bond angles and lengths for free oxazoline and oxazole ligands are shown in Tables 1 and 2.

In spite of the two C_{sp^3} at positions **4** and **5** (Fig. 1), the oxazoline cycle is nearly planar (the torsion angles **5**–**1**–**2**–**3** and **4**–**3**–**2**–**1** are 4.21 and 2.48°, respectively). However, it is less planar than the unsaturated oxazole cycle (the torsion angles **5**–**1**–**2**–**3** and **4**–**3**–**2**–**1** are ca. 1°), because of the sp^2 hybridization of **4** and **5** carbon atoms.

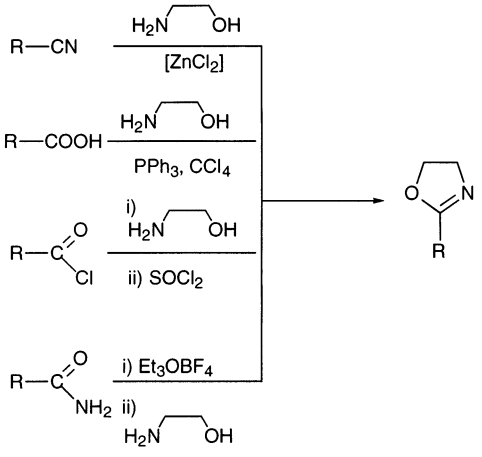

Scheme 1.

Table 1
Bond angles (°) mean values for oxazoline and oxazole free ligands (Fig. 1)

Ligand	**1–2–3**	**2–1–5**	**1–5–4**	**3–4–5**	**2–3–4**
Oxazolines[a]	118.39	105.70	103.56	103.98	106.85
Oxazoles[b]	113.41	104.96	107.38	109.38	104.84

[a] Mean values for 67 structures, 17 of which correspond to 2-aryloxazolines.
[b] Mean values for 38 structures, 14 of which correspond to 2-aryloxazoles.

The trend to ring planarity together with the value of the bond angle **1**–**2**–**3** (118.39°, which is nearly as great as the 120° for a sp^2 hybridization) and the similarity between the **2**–**1**–**5** and **2**–**3**–**4** angles (105.70 and 106.85°, respectively) (Table 1), suggest delocalization of the iminic double bond over three atoms (Scheme 2), as postulated elsewhere [12]. Nevertheless, the bond distances **2**–**3**, **1**–**2** and **1**–**5** are close to the average lengths for C_{sp^2}–N, C_{sp^2}–O and C_{sp^3}–O, respectively (Table 2). Therefore, it can be concluded that only a small contribution from the charged resonance structure (Scheme 2) is needed to describe the double bond on the oxazoline ring.

For 2-aromatic oxazolines in absence of steric hindrance (without *ortho* substituted phenyl groups), the ring tends to be coplanar with the phenyl group (the average torsion angle **3**–**2**–**6**–**7** is 4.27°). A planar conformation of the whole molecule was also calculated as being the most favorable [12c]. But the mean

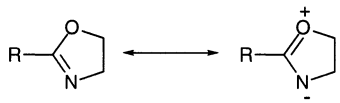

Scheme 2.

Table 2
Bond distance (Å) mean values for oxazoline and oxazole free ligands (Fig. 1)[a]

Ligand	**2–3**	**3–4**	**4–5**	**1–5**	**1–2**	**2–6**
Oxazolines	1.266 (1.28)[b]	1.474 (1.47)[c]	1.541 (1.54)[d]	1.451 (1.41)[e]	1.361 (1.34)[f]	1.462 (1.48)[g]
Oxazoles	1.294	1.395 (1.36)[h]	1.347 (1.34)[i]	1.377	1.364	1.470

[a] In parentheses, the average bond distances published [13].
[b] Mean double bond length for C_{sp^2}–N.
[c] Mean single bond length for C_{sp^3}–N.
[d] Mean single bond length for C_{sp^3}–C_{sp^3}.
[e] Mean single bond length for C_{sp^3}–O.
[f] Mean single bond length for C_{sp^2}–O.
[g] Mean single bond length for C_{sp^2}–C_{sp^2}.
[h] Mean single bond length for C_{sp^2}–N.
[i] Mean double bond length for C_{sp^2}–C_{sp^2}.

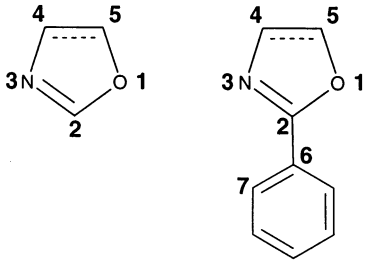

Fig. 1. 4,5-Dihydro-1,3-oxazoles (single bond between **4** and **5** carbon atoms) and 1,3-oxazoles (double bond between **4** and **5** carbon atoms).

distance **2**–**6** (1.462 Å) corresponds to a single bond C_{sp^2}–C_{sp^2}. So, C=N bond delocalization is not observed, either.

3. Metal transition complexes

The number of studies published in oxazoline chemistry is great. In the last two decades more than 200 papers have appeared analyzing the coordination compounds of these ligands. Most deal with the study of the intermediate metal species in catalytic processes, both in solution and solid state.

The crystal structures shown here are ball and stick representations using covalent atomic radii. Hydrogen atoms have been omitted.

3.1. Monodentate oxazoline ligands

Coordination complexes with the oxazoline ligands **N** shown in Chart 1 acting as monodentate were prepared.

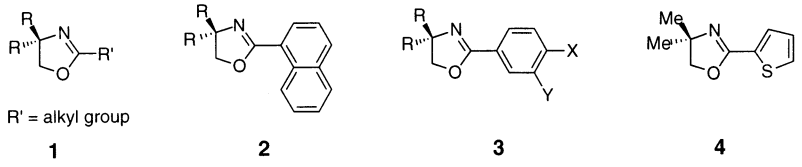

(Chart 1)

The reaction of metal salts with monodentate type **1** oxazoline ligands is straightforward and leads to the preparation of the corresponding coordination compounds. Hexacoordinate $[TiX_4(\mathbf{1})_2]$ compounds were prepared by reaction of **1** with TiX_4 (X = Br, Cl) [14]. From the IR spectroscopic data in the 400–240 cm^{-1} region, it may be inferred that these compounds have *cis* structures.

Regioselectivity studies of the cyclopalladation of naphthyl and phenyl oxazolines showed that the reaction of ligands **2** and **3** with Li_2PdCl_4 gives the $[PdCl_2(\mathbf{N})_2]$

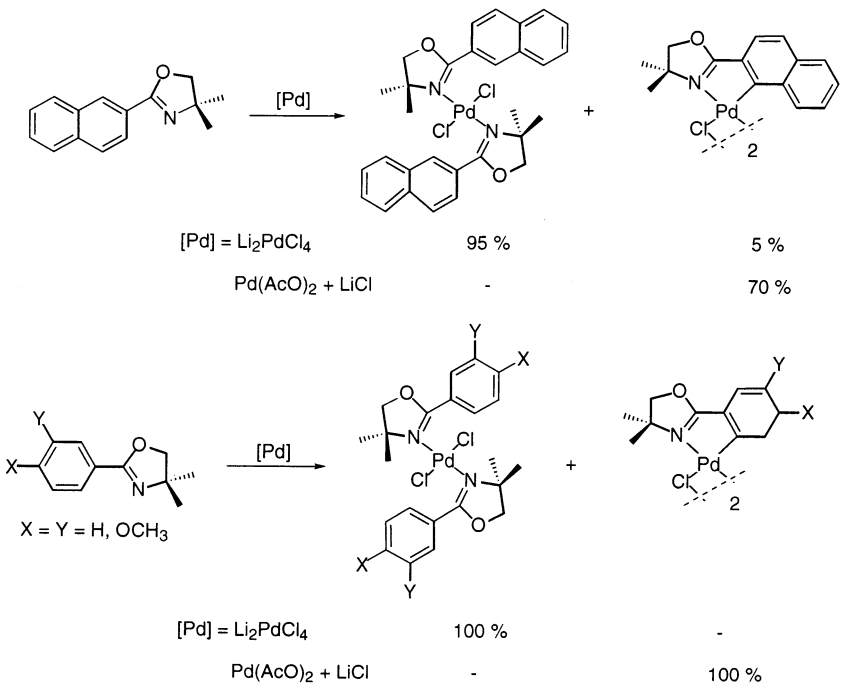

Scheme 3.

coordination complexes instead of the 3-palladated complex (Scheme 3) [15,16], although high yields of cyclometalated complexes are formed when $Pd(AcO)_2$ is employed.

The ^1H NMR spectrum of $[PdCl_2(\mathbf{2})_2]$ (R = Me) shows the presence of a *cis*/*trans* isomer mixture. Yet, only the *trans* isomer was crystallized (Fig. 2). The palladium center is almost perfectly square planar, surrounded by two *trans* organic ligands in an *anti*-fashion. The two oxazoline ligands are nearly orthogonal to the coordination plane with the naphthyl substituents tilted at 28.6° to the corresponding quasi-planar oxazoline ring.

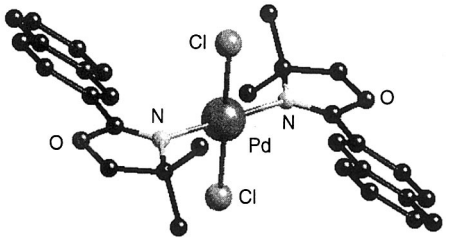

Fig. 2. Molecular structure of *trans*-$[PdCl_2(\mathbf{2})_2]$ (R = Me).

Oxazoline rings were obained directly from organonitrile ligands in transition metal complexes. Reactions of neutral [17,18] or cationic [19,20] nitrile complexes *cis*- and *trans*-$[PtCl_2(NCR)_2]$ (R = alkyl, aryl) and *trans*-$[Pt(R')(NCR)(PPh_3)_2]BF_4$ (R′ = H, CH_3, CF_3; R = alkyl, aryl) with organic nucleophiles like 2-chloroethoxide, generated either by deprotonation of 2-chloroethanol with a base or by ring opening of oxirane with Cl^- ion, yield imido ester [2-(R)-oxazoline] derivatives (Eq. (1)).

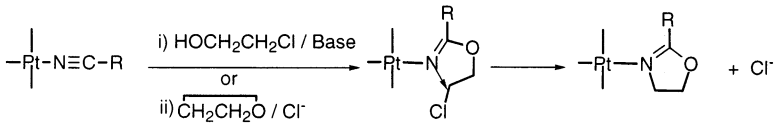

R = *p*-MeC_6H_4, *p*-$CF_3C_6H_4$, *o*-MeC_6H_4, Et, *n*-Pr, *i*-Pr, *t*-Bu. (1)

The reactivity of an alkyl and an aryl nitrile ligand do not differ, since the corresponding oxazoline complexes are obtained in comparable yields and with comparable reaction times. These complexes react with diphosphines to give free oxazoline, and the cationic complexes react with one equivalent of PPN^+Cl^- to give quantitatively free oxazoline (Eq. (2)) [19].

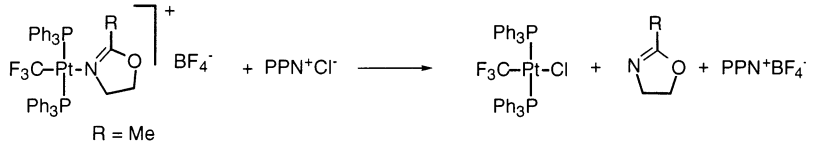

R = Me (2)

Structural data show that the coordination geometry around the Pt(II) atom is almost square-planar for the neutral *cis* (Fig. 3) and *trans* platinum compounds [17,18], but far from square-planar for the cationic complex *trans*-$[Pt(CF_3)(PPh_3)_2(\mathbf{3})]^+$ (X = Y = R = H) [19].

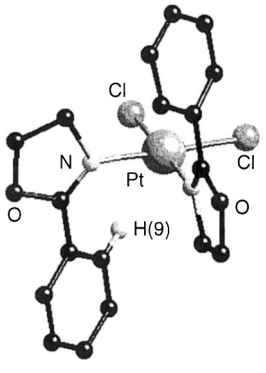

Fig. 3. Molecular structure of *cis*-$[PtCl_2(\mathbf{3})_2]$ (R = X = Y = H).

The five-membered rings of the two oxazoline ligands are nearly planar. This feature suggests that the hindrance posed by the substituent in position 2 has not effect on the geometry of the oxazoline moiety. In the *trans* neutral complex the coordination plane and the oxazoline ring are nearly perpendicular, thereby avoiding close intramolecular contact with the bulky *tert*-butyl group. In the *cis* complex the two oxazoline rings intersect the platinum coordination plane at different angles (95.7 and 88.2°), which is probably due to their varying steric requirements. The Pt–N bond distances for the two neutral compounds are comparable (2.011 Å), but they are shorter than those for the cationic complex (Pt–N distance 2.06 Å) where the CF_3 group is *trans* to the oxazoline ligand.

Neutral imine complexes can be produced by deprotonation of the aminooxycarbene (Eq. (3)). The coordinating ability of imine nitrogen is seen in its reaction with $[PdCl_2(NCMe)_2]$ [21].

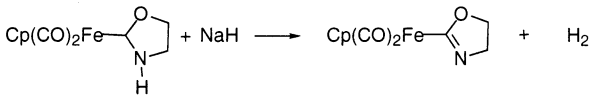

(3)

Similarly, monomeric rhenium complexes can be prepared, using *n*-BuLi as a deprotonating agent [22]. But the same reaction with platinum aminooxycarbene leads to the formation of the metalated dimeric species (Eq. (4)), the X-ray structure of which is shown in Fig. 4 [23].

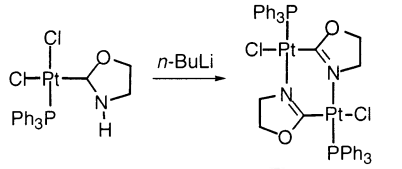

(4)

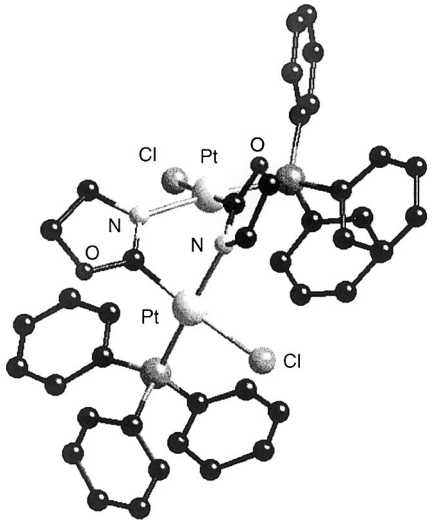

Fig. 4. Molecular structure of $[PtCl(PPh_3)\{\mu\text{-}COCH_2CH_2N\text{–}C,N\}]_2$.

The coordination geometry around each platinum atom describes an irregular square with deviations in the tetrahedral direction. The two coordination planes in the dimer are roughly orthogonally oriented. The hexaatomic ring formed by two Pt atoms and the nitrogen and carbon atoms of the bridging ligand has a boat conformation (where the apices are the metal ions), and the two phosphine ligands are oriented in opposite directions to the boat apices thereby minimizing molecular strain. The values found for the iminic bond (ca. 1.29 Å) are indicative of a substantial multiple bond character, with a significant π-bonding interaction, which involves not only the nitrogen and carbon atom but also the oxygen atom.

3.2. Bidentate mono(oxazoline) ligands

3.2.1. N,X-donor atoms (X = C, N, O, S)

3.2.1.1. N,C-donor atoms. Aryloxazolines, with various substituents on the aromatic ring, as well as alkyloxazoline ligands **1**, **2** and **3** (Chart 1) give cyclopalladated complexes on reaction with palladium acetate in acetic acid [15,16,24]. Oxidative addition of aromatic halides to palladium(0) complexes has been shown to provide an alternative pathway to aryloxazoline cyclopalladated compounds.

The reaction of different substituted aromatic oxazolines always leads to the formation of the dimeric species (Eq. (5)) and, when the formation of regioisomers is feasible, the isomer formed by palladation at the carbon atom suffering least hindrance is preferred.

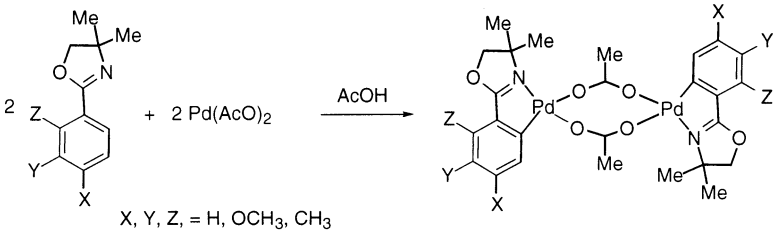

(5)

Steric hindrance around the amine group is not essential for this cyclometalation, since moving the *gem* dimethyl moiety from position 4 to 5 in the heterocyclic ring does not alter the yield [16,24]. The same reaction with alkyl oxazoline (2-*t*-butyl-4,4-dimethyl-2-oxazoline) not only gives a 62% yield of dimeric cyclopalladated complex but also a 16% yield of trinuclear species [25]. For the dimeric species, stereoisomerism is possible, involving *anti* and *syn* isomers. ^{1}H NMR data and crystal structure determination confirm that only the *anti* isomer is present. The temperature dependence of the spectra reveals fluxional behavior, indicating that exchange occurs for the *gem* methyl groups as well as for the methylene protons, presumably related to an interconversion between the two enantiomeric forms of the complex and involving a partial rupture of the acetate bridge. These cyclometalated complexes react with LiCl to give the chloro-bridging dimer, and with

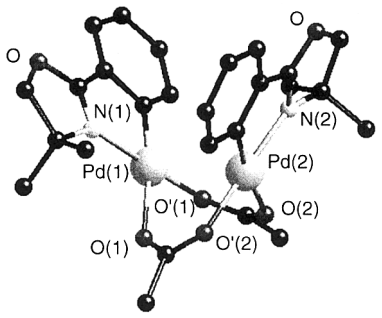

Fig. 5. Molecular structure for $[Pd(\mu\text{-AcO})(\mathbf{3})]_2$ (X = Y = H, R = Me).

pyridine, mono and diphosphines to give the monomeric species with the oxazoline ligand coordinated in a bidentate fashion. The reaction with iodoalkanes is perhaps of greater interest as it yields regioselectively 2- or 2,6-alkylated aryloxazolines [26], and it constitutes a simple, efficient method for preparing substituted aryloxazolines. A single-crystal X-ray determination was carried out for the dimeric complex $[Pd(\mu\text{-AcO})(\mathbf{3})]_2$ (X = Y = H, R = Me) (Fig. 5) [24]. It has an 'open book' type structure. A methyl group in each cycle is directed inwards while another is directed outwards, and so the molecule lacks elements of symmetry other than its C_2 axis and is therefore chiral. The coordination geometry around each palladium atom is approximately square-planar. The Pd–C distances are slightly shorter than expected for a covalent $Pd-C_{sp^2}$ bond, indicating a significant degree of metal to ligand back-bonding. The *trans* lengthening influence of a σ-bonded carbon is illustrated by the lengthening of the palladium oxygen distances *trans* to carbon atoms (ca. 2.12 Å) relative to those *trans* to nitrogen atoms (ca. 2.05 Å). The average bite angle for the metalated bidentate ligand is 81.0°, similar to that found in gold cyclometalated compounds [27].

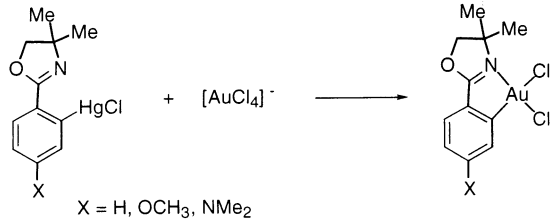

(6)

Chelated organogold(III) complexes can be prepared by transmetalation from the corresponding organomercury(II) compounds (Eq. (6)) [27]. Simple substitution of the chloro-complex for the stoichiometric amount of alkali-metal salts gave the corresponding bromo-, iodo- or thiocyanato-complexes. It is also possible to substitute a single chloride ligand by reaction with a small amount of DMSO or PPh_3, affording cationic complexes. The infrared spectra of the thiocyanate compounds suggest that they are S-bonded. The crystal structure of the chloro-complex *cis*-$[AuCl_2(\mathbf{3})]$ (X = H) was determined (Fig. 6). The gold atom has essentially

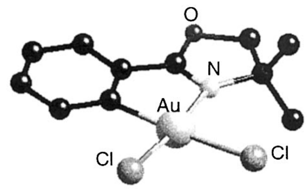

Fig. 6. Molecular structure of *cis*-[$AuCl_2$(**3**)] (X = Y = H, R = Me).

square-planar coordination, with the two Au–Cl bond lengths quite different. The Au–Cl bond, where the chlorine atom is *trans* to the phenyl group, is, as expected, the longest, on *trans*-influence grounds.

The oxazoline complexes decompose to metallic gold in the presence of silver acetate, even when light is rigorously excluded. The most interesting reactions of the chloro-complexes are with sodium dithiocarbamate, NaS_2CNEt_2. Even when the stoichiometry is strictly controlled at a ratio of 1:1, both chloride ligands are replaced; the single S_2CNEt_2 ligand chelates to gold(III), giving square-planar CNS_2-coordinated cations. The soft S_2CNEt_2 nucleophile binds to the gold directly, and does not attack the oxazoline group, which remains coordinated. Addition of a second S_2CNEt_2 ligand gives products that also retain the oxazoline group but that are bonded only by the carbon atom. Although the two dithiocarbamate ligands appear equivalent in the NMR spectra, one is probably monodentate and the other bidentate, with a rapid exchange ocurring between them.

Reaction of [AuCl(tht)] (tht = tetrahydrothiophene) with the lithium derivatives of **4** ligand, 2-(4′,5′-dihydro-4′,4′-dimethyl-2′-oxazolinyl)thien-3-yllithium or 2-(4′,5′-dihydro-4′,4′-dimethyl-2′-oxazolinyl)thien-5-yllithium gave thienyl dimeric and trimeric oligomers of gold(I) (Scheme 4), but when the gold(I) precursors were

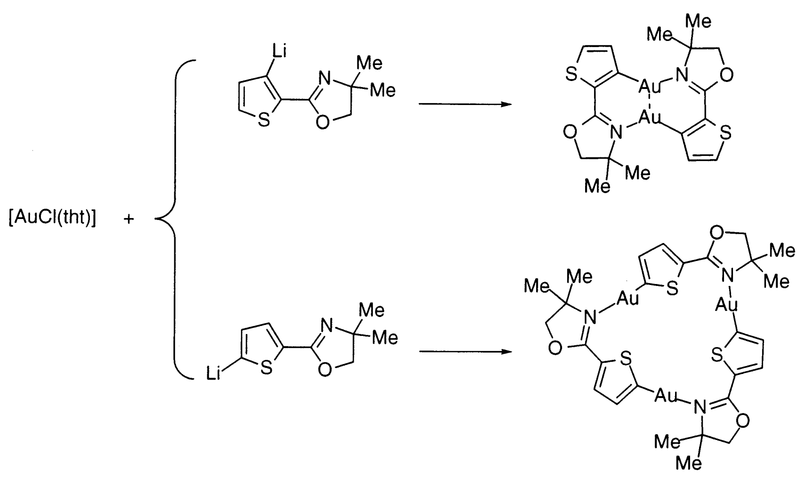

Scheme 4.

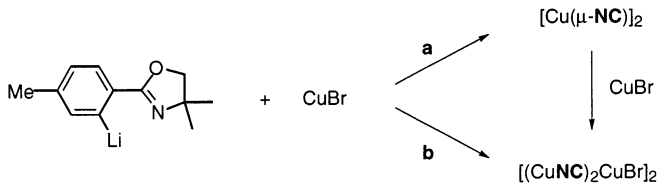

Scheme 5.

$[AuCl(PPh_3)]$ or $[Au(C_6F_5)(tht)]$, monometallic *N*-bonded complexes were obtained [28].

The molecular structure of the dimetallic complex (Scheme 4) shows that each gold atom is essentially linearly coordinated to a carbon atom of a (thienyl)-oxazoline ligand and to the nitrogen of a second oxazoline ligand thereby forming a cyclic binuclear Au(I) compound. No intermolecular Au···Au interactions occur. However, the gold atoms within the bicyclic compound are intramolecularly bound and exhibit a short separation of 2.85 Å. The aromatic character of the two thienyl rings is clearly shown by the planarity of the rings and the relatively short C–C (ca. 1.37 Å) and C–S (ca. 1.72 Å) bond lengths therein. In addition, the C–C bonds joining the thienyl and oxazolinyl rings are also shorter (ca. 1.46 Å) than normal single bonds. Moreover, the thienyl and oxazoline moieties lie in the same plane, indicating that π-delocalization occurs in the dimeric compound.

Organocopper compounds assist organic syntheses. A consideration of the mechanistic aspects of copper-mediated reactions often requires knowledge of the structures of the complexes. A convenient route for the synthesis of pure organocopper compounds is the reaction of an organolithium compound with CuBr. Lithiated aryl oxazolines can easily be prepared by direct low temperature metalation with *n*-BuLi in THF [29]. Arylcopper(I) complexes containing an oxazoline substituent at the *ortho* position to the Cu–C bond were synthesized from the corresponding aryllithium species and CuBr. Depending on the order of addition, this reaction afforded either a pure arylcopper(I) compound (slow addition of CuBr to the aryllithium reagent — path a in Scheme 5) or a mixture of arylcopper(I) and the $[(CuNC)_2CuBr]_2$ adduct (addition of aryllithium to a CuBr suspension — path b in Scheme 5) [1,30]. The ^1H NMR spectra of these complexes are temperature dependent, which is most probably due to the equilibrium between aggregated species.

The crystal structure of the arylcopper dimer $[Cu(\mu\text{-}NC)]_2$ (Fig. 7) indicates that the two oxazolinyl groups act in bidentate fashion bridging the two copper atoms, each of which is bonded via a two-center, two-electron bond to C_{ipso} of an aryl ring and to the nitrogen atom of the oxazoline substituent [31].

The copper atoms are coordinated almost linearly (N(1)–Cu(1)–C(1) = 177.8°), but the N(1)–Cu(1)–C(1) and N(2)–Cu(2)–C(2) axes are not parallel and the oxazoline substituent is rotated out of the plane of the aryl groups to which it is bonded. The structural features of binuclear arylcopper differ from those usually found in arylcopper compounds: organocopper complexes are characterized by

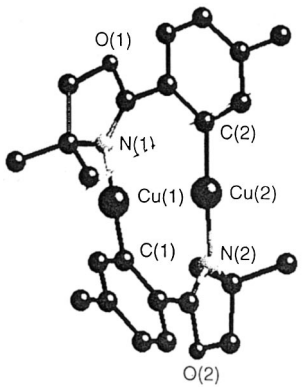

Fig. 7. Molecular structure of $[Cu(\mu\text{-}\mathbf{NC})]_2$.

their high degree of aggregation and the presence of copper–carbon bonds in the multicenter bonding of a three-center, two-electron type. The difference in behavior can be ascribed to the special requirements of the oxazolinylaryl ligand, i.e. the orientation of the lone pair of the N heteroatom and the steric bulk of the oxazoline substituent of the aryl system. Replacement of a 2-(2-oxazolinyl)aryl group by a stereochemically less demanding Br atom allows for a higher degree of aggregation, as is reflected in the formation of the hexanuclear structure $[(Cu\mathbf{NC})_2CuBr]_2$. This polynuclear species (Fig. 8) has a structure comprising six Cu atoms positioned at the apices of a distorted octahedron.

There are two types of Cu atoms with a different number of interactions with the ligands: the apical atoms (Cu(1)) are coordinated exclusively to C_{ipso} atoms while the equatorial atoms (Cu(2)) are bonded to C_{ipso}, Br and N atoms. Three-center, two-electron bonded aryl groups bridge a copper atom pair which lie almost

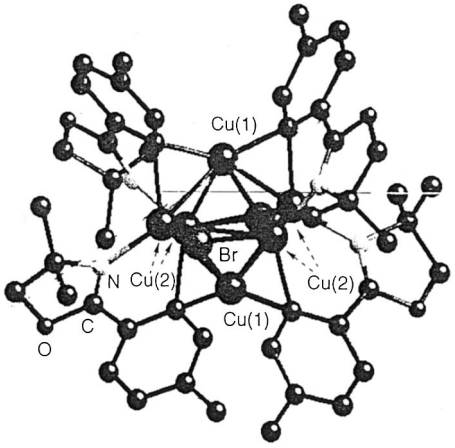

Fig. 8. Molecular structure of $[(Cu\mathbf{NC})_2CuBr]_2$.

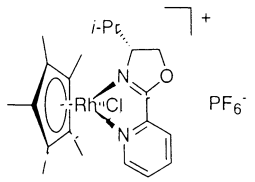

Fig. 9.

perpendicularly to the copper–copper axis. The bromine atoms symmetrically bridge two copper atoms in the equatorial plane of the octahedron, and the oxazoline group is coordinated via the nitrogen atom to the equatorial Cu atoms.

3.2.1.2. N,N′-donor atoms. **NN′** ligands, such as substituted (2-pyridin-2-yl)-2-oxazoline (**5**) (Chart 2), were used as chiral auxiliaries in the preparation of enantiomerically pure chiral ruthenocenes [RuClCp*(**NN′**)] from mixtures of $[RuClCp^*]_4$ and the oxazolinic ligand. A 1:10 ratio of diastereomer mixture was obtained [32].

(Chart 2)

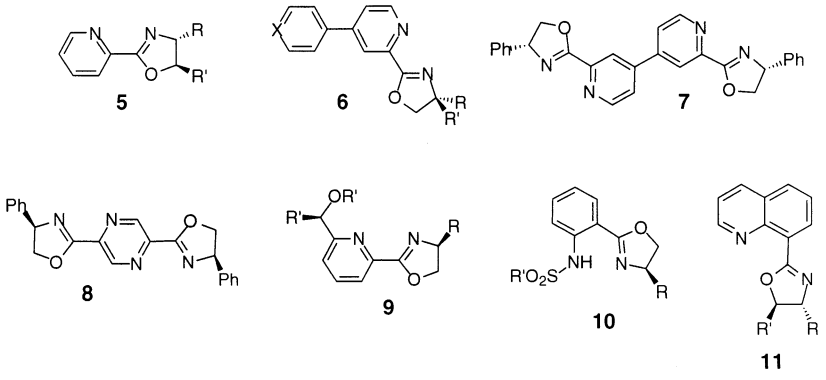

The same kind of half-sandwich rhodium oxazoline complexes (Fig. 9) was synthesized and used in asymmetric Diels–Alder reactions. The complexation is highly diastereoselective and only one diastereomer was observed by ^1H NMR spectroscopy. The bite angle N–Rh–N′ is 76.0°, and the distances $Rh–N_{pyridine}$ and $Rh–N_{oxazoline}$ are 2.142 and 2.109 Å, respectively. In the symmetrical complex with a bis(oxazoline) (type **37**), the distances Rh–N are 2.117 and 2.157 Å, but in this case in a six-membered metalocycle [33].

Bidentate ligands built by combining an imidazoline-2-ylidene group and a chiral oxazoline were used to obtain rhodium and palladium carbene complexes (Eqs. (7–9)).

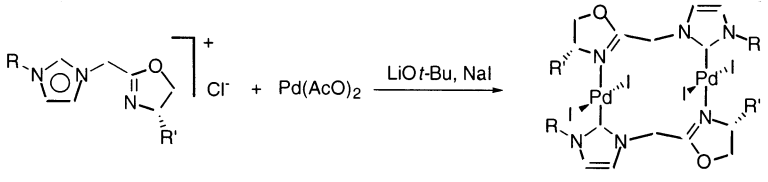

(7)

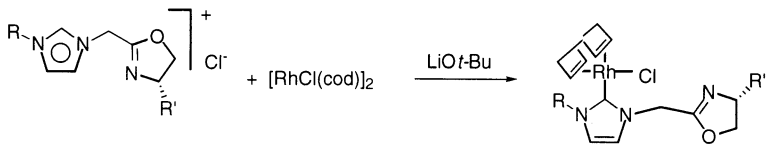

(8)

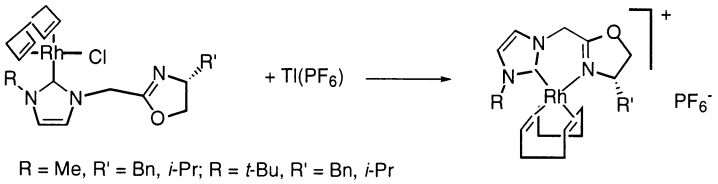

R = Me, R' = Bn, *i*-Pr; R = *t*-Bu, R' = Bn, *i*-Pr

(9)

The distances between the Rh atom and the olefin *cis*-1,5-cyclooctadiene double bonds suggest that carbene is a stronger donor than oxazoline (Eq. (9)). The crystal structure determination of the palladium compound (Eq. (7)), with R = Me and R′ = *i*-Pr, confirmed their binuclear nature [34].

The synthesis of 2-(4,4′-bipyridin-2-yl)-oxazolines, 2-(4′-phenylpyridin-2′-yl)oxazolines and 4,4′-bipyridine- or pyrazine-bis(oxazolines) (**6**–**8**) and the preparation of certain Rh(I) complexes from type **6** (X = N, C) and **7** ligands were reported [35].

The [Rh(cod)(**6**)]PF_6 or [Rh_2(cod)$_2$(**7**)](PF_6)$_2$ complexes revealed the ligands to be coordinated in a bidentate fashion. The proton in *ortho* position in the pyridine moiety exhibited a strong downfield, 0.87 ppm, from the free ligand. Both the ^{1}H and ^{13}C NMR spectra showed significant differences depending on the anion BF_4^- or PF_6^- in the [Rh(cod)(**NN′**)]Y compound. The distances Rh-double bond in *trans* position to the pyridine or the oxazoline fragments are 2.025 and 1.995 Å, respectively.

Twenty-one pyridyl–oxazolines (type **5**) were obtained for testing in the hydrosilylation reaction, using [Rh(cod)(**5**)]PF_6 as catalyst precursor [36]. These complexes are relatively stable, both in solid state and solution (Fig. 10).

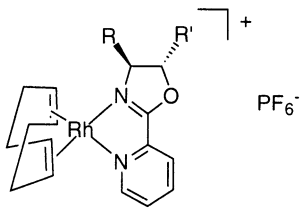

R = Et; R' = H
R = CH_2OH; R' = Ph

Fig. 10. Pyridine–oxazoline rhodium(I) complexes.

A group of octahedral neutral and ionic nickel compounds $[NiX_2(\mathbf{5})_2]$ (X = Cl, Br, NCS) and $[Ni(H_2O)_2(\mathbf{5})_2](ClO_4)_2$ (**5**, R = R′ = CH_2OH, CH_3; R = CH_3, R′ = CH_2OH) were characterized by analytical data, vibrational and electronic spectroscopy and magnetic moment values [37].

The modulation of the asymmetric induction of the pyridyl–oxazoline ligands with their chiral center in the oxazoline fragment in catalytic applications is difficult to evaluate, since the different *trans* influences from the different ligand donor atoms must also be considered. Chelucci reported the preparation of four new *ortho*-methyl pyridyl–oxazolines [38], while Moberg et al. [39] obtained a group of 13 pyridyl–oxazoline ligands (**9**) with chiral centers in both oxazoline and pyridine fragments in order to evaluate this effect accurately. The enantioselective allylic substitution reaction catalyzed by palladium complexes with these ligands was studied. Two complexes $[Pd(\eta^3\text{-}C_3H_5)(\mathbf{NN}')]PF_6$ were obtained and their 1D and 2D spectra analyzed.

In our laboratory, allylic palladium complexes with pyridyl- and quinolinyl–oxazolines (**5** and **11**, respectively), $[Pd(\eta^3\text{-allyl})(\mathbf{NN}')]PF_6$, were synthesized and characterized [40]. Due to the presence of substituents on the oxazoline moiety, two isomers (*exo* and *endo*) can be distinguished, where *endo* refers to the finding that the central allylic carbon points away from the oxazoline substituent nearest the N atom (Eq. (10)).

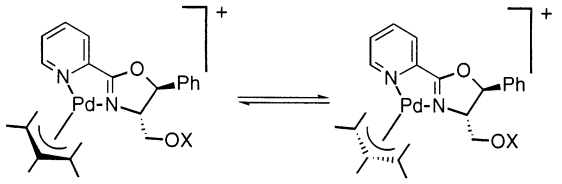

endo *exo*

X = H, Me, Ph, CPh_3 (10)

Variable temperature NMR spectra exhibited fast interchange between the isomers in coordinating solvents (acetone, acetonitrile), even at low temperatures. On the NMR time scale, palladium-allyl rotation seems to be faster than η^3-η^1-η^3 movement. But with non-coordinating solvents (such as chloroform), the two isomers were observed in an unchanged ratio of 3:2. Presumably, the isomer ocurring at a greater ratio corresponds to the less hindered *endo* complex, the structure of which was determined by X-ray diffraction (Fig. 11; **5**, R = CH_2OCPh_3 and R′ = Ph). The bond distances Pd–C(1) and Pd–C(2) are 2.134 and 2.098 Å, respectively, showing a slight difference in the *trans* influence between the two nitrogen atoms. In allylic substitutions, palladium quinolinyl–oxazoline (**11**) systems show higher catalytic activities and enantioselectivities than those shown by analogous pyridyl–oxazoline (**5**) precursors. This behavior might be explained by the effect of the metal ring size, which ensures that the substituent on the chiral carbon near oxazolinic nitrogen is closer to the allyl substrate in quinolinyl–oxazoline complexes. The NOESY spectrum of $[Pd(\eta^3\text{-allyl})(\mathbf{11})]PF_6$ (**11**, R = CH_2OH

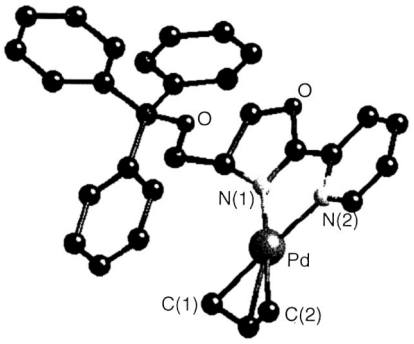

Fig. 11. Molecular structure of $[Pd(\eta^3\text{-}C_3H_5)(\mathbf{5})]PF_6$ ($R' = Ph$, $R = CH_2OCPh_3$) The hexafluorophosphate anion and the phenyl group on the oxazoline ligand have been omitted for clarity.

and $R' = Ph$) shows nuclear Overhausser interaction between one hydrogen *syn* of the allyl fragment and the hydrogen *ortho* to quinoline nitrogen. However, this NOE effect does not occur for analogous pyridine derivatives because of the long interatomic distance (> 3.6 Å for hydrogen *syn* of the allyl fragment and the hydrogen *ortho* to pyridine nitrogen [41]).

Palladium(II) and platinum(II) diaqua(2-pyridin-2-yl)-2-oxazoline (**5**) dications react with model nucleobases to give binuclear complexes. The platinum compound $[PtCl_2(\mathbf{NN}')]$ was tested in its antitumor activity. The crystal structures of the binuclear complexes shown in Fig. 12 were determined. These complexes seem to be unstable in aqueous solution, as indicated by ^{1}H NMR studies [42].

Stable neutral copper(II) complexes (Fig. 13) were obtained from substituted anionic sulfonylamino–oxazolines (**10**) [43]. These complexes are precursors of catalytic species active in the asymmetric cyclopropanation of olefins.

3.2.1.3. N,O-donor atoms. Several substituted phenoloxazoline compounds (**NOH**, Chart 3) become good bidentate monooxazoline ligands (**NO**) after deprotonation. Reaction of metallic salts, usually containing basic anionic ligands such as acetate and acetilacetonate or even halides, with phenoloxazoline affords compounds with coordination numbers four, five or six.

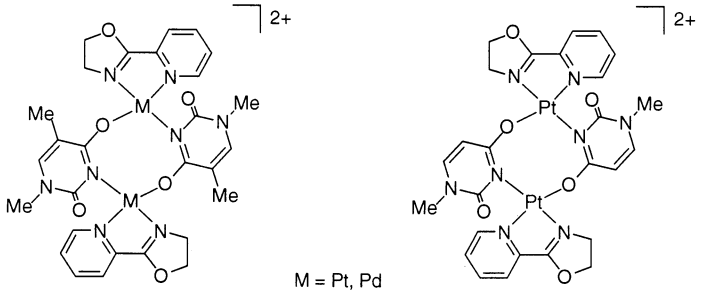

Fig. 12. Bimetallic dications with pyridine–oxazoline ligands [42].

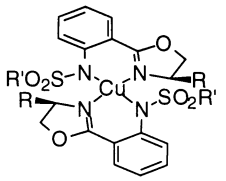

Fig. 13.

(Chart 3)

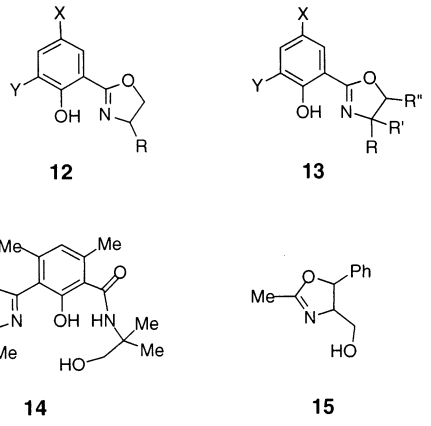

12 **13**

14 **15**

Tetracoordinate [M(**NO**)$_2$] complexes were obtained with **NO** ligands **12** and **13**, each showing different alkyl and aryl substituents in X, Y, R, R′ and R″ positions, and M = Cu, Zn, Ni, Co, Fe, Pd, Mn [44–46]. Some of the diamagnetic complexes were characterized in solution by NMR spectroscopy revealing that whereas the palladium complex [Pd(**12**)$_2$] (X = Y = H, R = Et) only showed the *trans* isomer, the analogous nickel complex showed two isomers (*cis* and *trans*) with a major:minor ratio 2:1. The *trans* is probably the major isomer. Exchange between the two isomers cannot be appreciated by NMR variable temperature experiments [45]. X-ray structural studies conducted with [M(**12**)$_2$] compounds show that the similar donor atoms N, N and O, O are *trans* to each other. This arrangement means molecules orient the substituent groups on the oxazoline ligands to the same side of the molecular plane, as shown in the crystal structure of various metal complexes. In all these complexes the oxazoline heterocycle is nearly planar and the angle between the phenyl ring and the six-membered metallic cycle is very small, so the two six-membered rings are nearly coplanar. Figs. 14–16 show the crystal structure of complexes [M(**12**)$_2$]. The coordination geometry around the central ion in palladium complexes is essentially square-planar, as shown in Fig. 14, while the nickel complex shows distorted square-planar geometry tending to a tetrahedral configuration. Fig. 15 shows that the Zn atom in [Zn(**12**)$_2$] has a distorted tetrahedral coordination configuration. The planes between the benzene ring and the heterocycle are only slightly twisted.

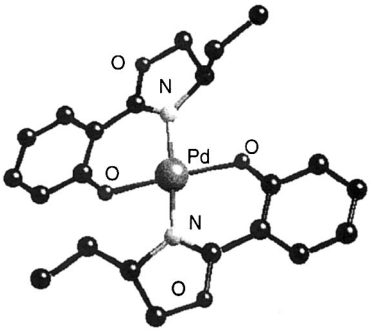

Fig. 14. Molecular structure of [Pd(**12**)$_2$] (X = Y = H, R = Et).

The copper atom of the complex shown in Fig. 16 has a distorted square pyramidal configuration; it becomes pentacoordinated because of the interaction between the Cu atom and the O atom of the phenolato ligands of the adjacent molecule (Cu(2)–O(1)), affording a pseudodimeric species [44]. The bite angle for [M(**12**)$_2$] complexes varies from 90.2 to 95.2°, with the biggest angle being that for the tetrahedral Zn complex.

Several tetracoordinate complexes type [MLL′(**NO**)] were prepared. Reaction of [PdCl(acac)(PPh$_3$)] with the chiral ethyloxazoline **12** (X = Y = H) gave the compound [PdCl(**NO**)(PPh$_3$)] [45]. The complex exhibits an almost square-planar geometry with the nitrogen and phosphorus atom in *trans* position. The greater *trans* influence of the PPh$_3$ ligand is clearly observed; the bond distance Pd–N is 2.051 Å, whereas in the bis(phenolatooxazoline) complex shown in Fig. 14 it is in the range 1.99–2.01 Å. When L and L′ ligands are organic groups the synthesis is usually based on the fast reaction of bridging ligands in dimeric organometallic species with phenoloxazoline molecules. The reactivity of dimeric μ-hydroxonickel species was studied [45], as shown in Scheme 6.

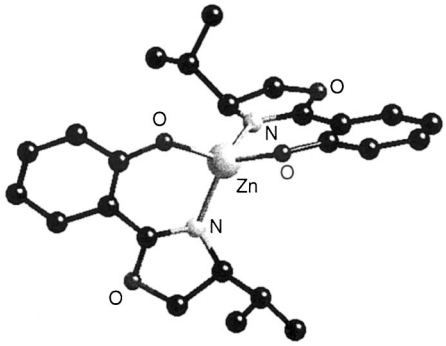

Fig. 15. Molecular structure of [Zn(**12**)$_2$] (X = Y = H, R = *i*-Pr).

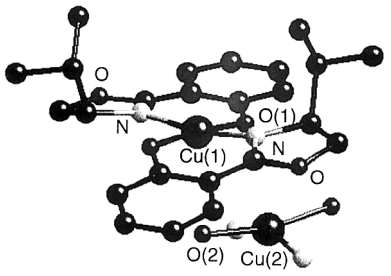

Fig. 16. Molecular structure of [Cu(**12**)$_2$] (X = Y = H, R = *i*-Pr) with a fragment of a second molecule showing the pseudo-pentacoordination of Cu(1) by the atom O(2).

For the paramagnetic pentacoordinate nickel complex the magnetic susceptibility value at room temperature (r.t.) ($\mu_{eff} = 3.22\ \mu_B$) corresponds to two unpaired electrons with a large orbital contribution. For the organometallic complex, the ^{19}F NMR spectrum shows the signals of two different C_6F_5 groups according to a *cis* configuration. The same reactivity was tested with hydroxopalladium species, but it was not possible to separate the organometallic compounds as had been expected. However, when the reaction was performed with bridging acetate or bromine precursors in the presence of a base such as DBU or *n*-BuLi, several organometallic complexes were obtained [45]: [Pd(CN)(**12**)] (where CN is a cyclometalated imine), [Pd(Mes)(**12**)(PPh_3)] (Mes = mesitylene) and allylic compounds [Pd(η^3-2-Me-C_3H_4)(**12**)] (**12**, X = Y = H, R = Et). ^1H NMR spectra revealed the absence of a symmetry plane in the coordination sphere due to the chiral oxazoline ligand: in the mesitylene complex the two *o*-methyl and the two phenyl protons of the mesitylene ligand appeared with different chemical shifts. Moreover, the allyl compound was obtained as a mixture of the *exo* and *endo* isomers. Nicholas and co-workers [47] prepared and characterized a series of [Pd(η^3-cyclohexenyl)(**NO**)] with chiral **NO**

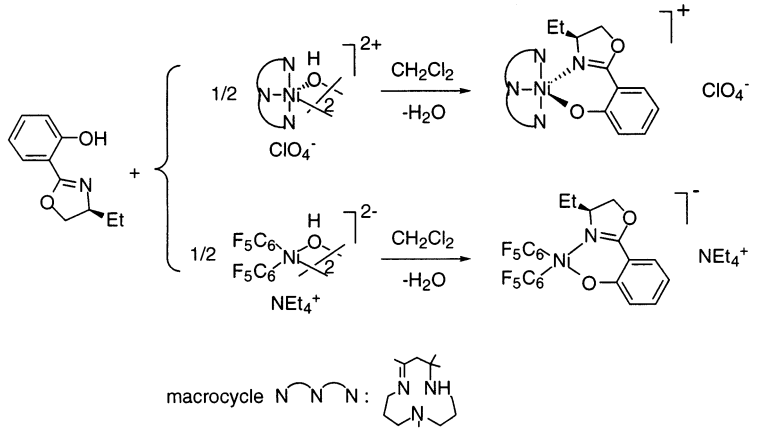

Scheme 6.

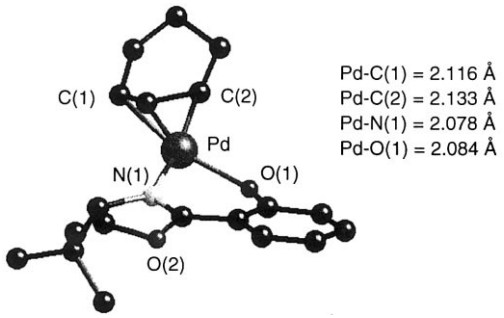

Fig. 17. Molecular structure of [Pd(η^3-cyclohexenyl)(**12**)] (X = Y = H, R = *t*-Bu).

ligands **12** in assessing their potential as an intermediate model for regio- and stereocontrolled catalytic oxidation and substitution reactions (Eq. (11)).

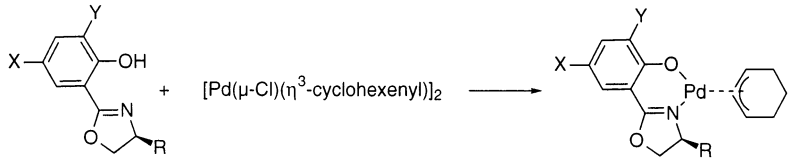

As expected, ^{1}H NMR spectra reveal the presence of a mixture of *endo* and *exo* isomers at different ratios depending on the size of the R substituent. While phenyl derivative has a 1:1 ratio, the *tert*-butyl derivative has essentially just one isomer (95%) in solution. The NMR spectra remain unchanged during variable temperature experiments, indicating that isomer interconversion is slow. That Pd–allyl rotameric equilibrium can be controlled via manipulation of the 2-position substituent on the oxazoline ring demonstrates the potential for influencing the binding stereochemistry of the substrate at the metal center of such complexes. The terminal allylic proton resonances are separated (ca. 0.5 ppm), indicating a significantly different environment. Fig. 17 shows the molecular structure of the phenolatooxazoline palladium cyclohexenyl complex. The geometry around the Pd atom is approximately square-planar, as defined by O(1), N(1), C(1), C(2). Pd–C terminal allyl bond lengths are almost identical. The N(1)–Pd–C(1) and O(1)–Pd–C(2) angles are nearly equal, indicating little or no difference in the *trans* influence of the N and O ends of the chelate. X-ray diffraction demonstrates that the *tert*-butyl group and the cyclohexenyl flap are *exo*.

Reaction of [V(O)(acac)$_2$] with **12** ligands (X = Y = H, R = *i*-Pr, Et) gives the pentacoordinate complexes *trans*-[V(O)(**NO**)$_2$]. When the more demanding substituents were present in the aryl and oxazoline groups (Y = R = *t*-Bu, X = H, NO_2), the corresponding vanadium complexes could not be prepared when reaction times were prolonged [48], but a tetracoordinate copper(II) complex was prepared with this bulky ligand [49]. The pentacoordinate vanadium complexes (Fig. 18) have a square-pyramidal coordination with the oxazoline N and phenolato O atoms

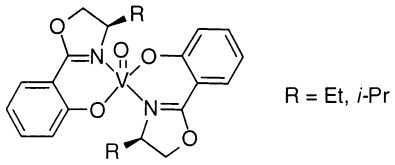

Fig. 18. Square-pyramidal coordination in vanadium complexes.

located in an almost *trans* planar arrangement with the phenolato oxazoline ligand being nearly planar. In both complexes the vanadyl oxygen atom is on the same side as the oxazoline substituents. The bulky methyl groups at the termini of these substituents point out the outer sphere of the complexes. The bite angle for these complexes (85.2 and 86.4°) is smaller than that in the tetracoordinated compounds $[M(\mathbf{NO})_2]$ described above.

Hexacoordinate complexes type $[MLL'(\mathbf{NO})_2]$ were prepared with different metals, different oxidation states and two bidentate ligands in the coordination sphere. But, tris-ligand transition metal complexes $[M(\mathbf{NO})_3]$ were scarce. Recently, manganese(III) complexes $[Mn(\mathbf{NO})_3]$ have been described with phenolatooxazoline ligand **12** (R = H) without any substituent on the heterocyclic ring [50]. Its structure consists of an octahedrically based Jahn–Teller distorted *mer*-$[Mn(\mathbf{NO})_3]$ species with bite angles varying from 85.05 to 88.37°. Koikawa et al. [51] synthesized the phenolatooxazoline ligand **14** (Chart 3) which reacts with Mn(III) acetate, yielding the compound $[Mn(AcO)(\mathbf{14})_2]$. The structure of the complex is characterized by the presence of non-coordinating amide and hydroxyl groups in the aliphatic chain.

The deprotonation of phenoloxazoline with NaH gives a THF solution salt, which reacts in situ with metal chlorides and leads to stoichiometric complexes $[MCl_2(\mathbf{NO})_2]$ and $[MCl(\mathbf{NO})_2(THF)]$ [52] (Scheme 7).

All these complexes were fully characterized, with X-ray structure determinations being performed for several of them. Titanium and zirconium complexes have a *cis* arrangement of the two functionalizable sites, which is particularly important for metal-assisted organometallic transformations. The six-membered chelated rings are quasi-planar and nearly perpendicular to each other. Moreover, the oxazolinato ligand appears to be almost planar. For titanium(III) complex, the Ti–Cl bond is

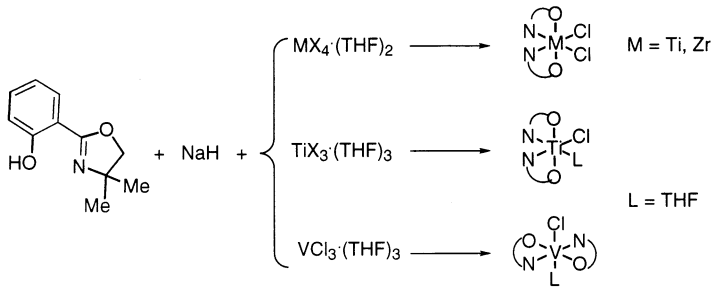

Scheme 7.

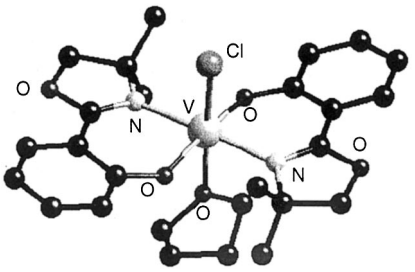

Fig. 19. Molecular structure of [VCl(**13**)$_2$(THF)] (X = Y = R″ = H, R = R′ = Me).

longer (Ti–Cl = 2.424 Å) than that in titanium(IV) compound (Ti–Cl = 2.319 Å). In vanadium(III) complex [VCl(**13**)$_2$(THF)] (Fig. 19), the two oxazolinato ligands arrange their donor atoms in a *trans*-planar configuration. Coordination is completed by a chlorine atom and a THF molecule *trans* to each other. The methyl groups of the planar oxazolinato ligands are arranged almost symmetrically with the coordination plane.

Organometallic complexes of titanium and zirconium were not obtained by reaction of [MCl$_2$(**NO**)$_2$] M = Ti, Zr with organolithium (MeLi) or organomagnesium (MeMgBr) reagents. However, direct alcane elimination from [M(CH$_2$Ph)$_4$] and **13** ligands gives dibenzyl complexes [53]. Room temperature ^{1}H NMR spectra suggest that, in solution, the neutral organometallic complexes contain two η^1-CH$_2$Ph groups, indicated by the absence of high field shift for the *ortho* protons and by AB splitting for the diastereotopic methylene protons. Fig. 20 shows the X-ray structure of the zirconium dibenzyl complex *cis*-[Zr(CH$_2$Ph)$_2$(**13**)$_2$]. The structural parameters (M–O and M–N bond distances and associated angles) do not allow a significant π-interaction of the zirconium with the donor atoms of the ligand to be considered.

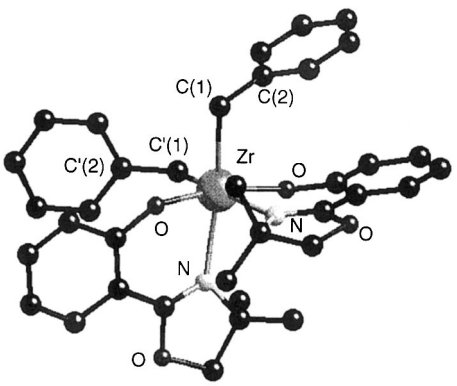

Fig. 20. Molecular structure of *cis*-[Zr(CH$_2$Ph)$_2$(**13**)$_2$] (X = Y = R″ = H, R = R′ = Me).

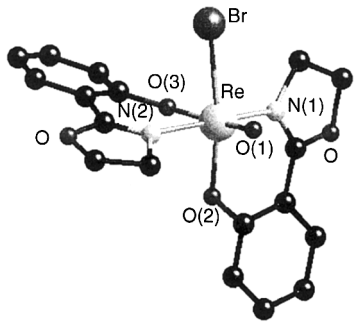

Fig. 21. Molecular structure of [ReBr(O)(**12**)$_2$] (X = Y = R = H).

By reaction with preformed M=O cores and the phenolatooxazoline ligand **12** (Chart 3, X = Y = R = H; X = R = H, Y = Me), a series of neutral oxotechnetium(V) and oxorhenium(V) complexes of general formula [M(O)X(**NO**)$_2$] (X = halide) were prepared [54]. The ^{1}H NMR spectra of these complexes are indicative of the two ligands in different chemical environments (i.e. a *cis* arrangement). Higher temperature NMR spectra showed decomposition before fluxionality. The crystal structure of [ReBr(O)(**12**)$_2$] (Fig. 21) shows that one ligand coordinates in the equatorial plane to Re=O, while the second ligand has its phenolate oxygen atom bound axially and its oxazoline nitrogen atom bound equatorially with respect to the oxobond.

The Re=O bond distance is 1.681 Å, which is typical of a rhenium–oxygen double bond. The Re–O(3) bond length of 1.988 Å is consistent with the *trans* influence for oxygen from an axially bound ligand *trans* to the Re=O linkage. In the equatorial plane, the two nitrogens coordinate *trans* to one another, while the bromine is *trans* to the equatorial coordinated oxygen. The bond angles show that the rhenium complex is closer to a perfect octahedron, with an O(3)–Re–N(2) bite angle of 90.0° for the equatorial ligand and a O(2)–Re–N(1) angle of 81.5° for the axial and equatorial ligands. Several general conclusions on the structural features of this hexacoordinated bis(ligand) complexes can be drawn: all of them show a single isomer in the solid state, the geometry around the metal center is a distorted octahedron, the two oxazolinato ligands are almost planar, mutually orthogonal and in a *cis* position except for the *trans* vanadium(III) complex. The bite angles of these complexes are very similar, varying from 77 to 87°. As such they are smaller than those recorded in tetracoordinate and pentacoordinate bis(oxazolinato) complexes described above. Bond distances within the oxazoline ligands correspond to a double bond mainly located between the N and C atoms. The bond parameters do not depend on the substituents on the oxazoline ring but on the nature of the metal atom, the oxidation number and on the other ligands coordinated with the central ion.

Reaction of a methanolic copper(II) acetate solution of enantiomerically pure (5*R*)- or (5*S*)-methyl-*E*-(4-ethyl-2-oxazolidiylidene)cyanoacetate leads to the mononuclear chelate (*RR*) or (*SS*) complexes (Eq. (12)) [55].

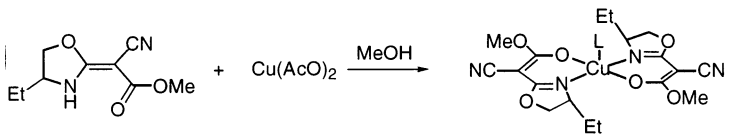

L = MeOH (12)

The X-ray crystal structure of the *RR* complex shows that the copper(II) center has a slightly distorted tetragonal pyramid geometry because of coordination of two anions of the ligand and one methanol molecule. The bond distance of the central copper atom to the enolato oxygens and oxazoline nitrogens (Cu–O = 1.98, 1.96 Å; Cu–N = 1.92, 1.93 Å), that form the tetragonal plane, is very similar to that found in phenolatooxazoline complexes type [Cu(**NO**)$_2$] described in Fig. 16. Methanol occupies the least hindered axial position with a Cu–O distance of 2.264 Å. Recrystallization of (*RR*) or (*SS*) mononuclear chelate complexes from non-coordinating chloroform and asymmetric induction via the stereogenic centers, stereospecifically yields the right- and left-handed helical 1D-coordination polymers. X-ray crystal structure analysis clearly demonstrates a well-ordered infinite 1D architecture. The available structures reveal that each of the copper atoms are linked across the nitrogen atom of only one neighboring cyano group of monomers. The central copper atoms are almost tetragonal-pyramidally coordinated, with the planes of the two ligands **NO** twisted from each other to an angle of 24.8°. The monomers are not perpendicular to each other in the helix polymer. It should be noted that the bite angle of the bidentate ligand does not change from the monomeric to the polymeric form. Indeed, both are close to the 90° found in other tetracoordinated bis(phenolatooxazoline) ligand complexes [44].

The cluster [Ru$_3$(CO)$_{12}$] reacts with (4*S*,5*S*)-(−)-2-methyl-5-phenyl-2-oxazoline-4-methanol **15** (Chart 3) to give [Ru$_6$(H)$_2$(CO)$_{14}$(**15**)$_2$] [56]. The molecular structure is shown in Fig. 22.

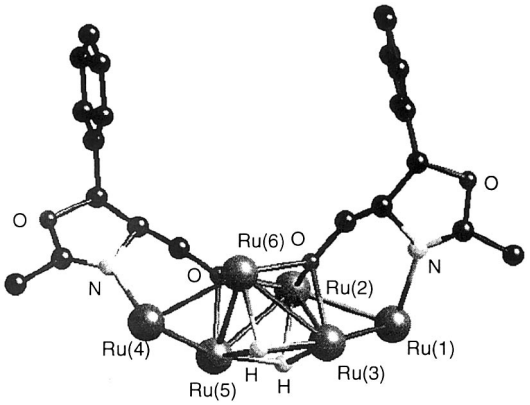

Fig. 22. Molecular structure of [Ru$_6$H$_2$(CO)$_{14}$(**15**)$_2$] without CO for clarity.

The metal core can be described as being formed by two triangles Ru(1)/(2)/(3) and Ru(4)/(5)/(6) with weak interactions between their two edges. The average Ru–Ru distance within the triangles is 2.752 Å and between the triangles is 3.061 Å. Each **NO** ligand coordinates to four metal atoms, with the ring nitrogen atom and the alcoholate function coordinating with one and three ruthenium atoms, respectively. The equivalence of two hydrides is observed in the crystal structure and is also evident from the ^{1}H NMR spectrum, which shows only one sharp signal in the metal hydride region at -11.6 ppm and does not change within the temperature range of $+20$ to -70°C.

3.2.1.4. N,S-donor atoms. Mixed sulfur–nitrogen ligands of the type thioether–oxazoline (**NS**), **16–18,** (Chart 4) were prepared and used as chiral auxiliaries in palladium catalyzed allylic substitution [57]. The results indicate that aryl sulfides provide higher levels of enantioselectivity than are provided by alkyl sulfides. The best asymmetric induction properties were observed with the ligands that force a six-membered chelate ring (**16**, **18**) and that are more rigid (**16**). The best ligands of type **16** (including sulfoxides) were studied in detail [58], and tested in the same reaction with excellent conversion and in some cases good enantioselectivity. The asymmetric induction was found to be highly dependent on the substituent attached at sulfur atom.

(Chart 4)

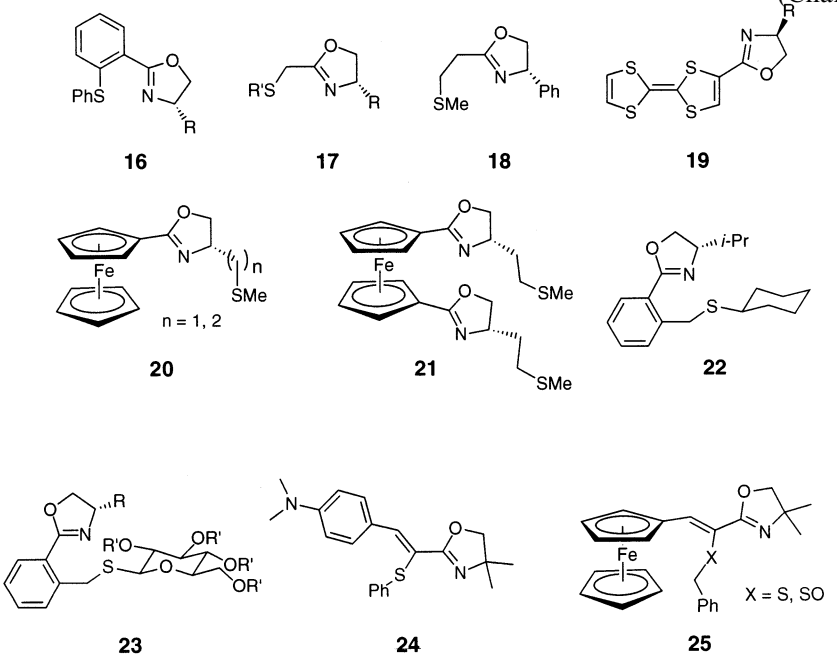

When chiral oxazolines linked to the tetrathiofulvalene group (**19**) were also used in the palladium catalyzed allylic substitution, the enantiomeric excess was lower than for ligands **16–18** [59]. This could be due to the different π-acceptor character

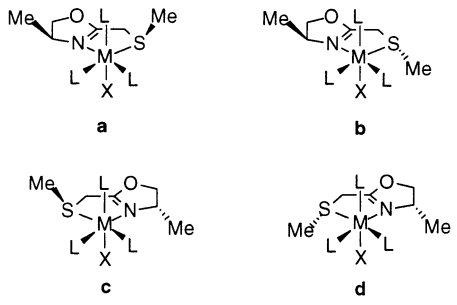

Fig. 23. Diastereomers for the *fac*-[MXL_3(**17**)] complexes.

of the sulfur atoms, greater in ligands **16–18**, which directs the nucleophilic attack *trans* the sulfur atom and gives better enantioselectivities. The best results were obtained with ferrocenyl–oxazolines incorporating thioether units (**20**, **21**) [60]. In this case, greater stability of the palladium complexes containing a six-membered metalocycle could be observed. The conversion and selectivity of the catalytic reaction are greater with ligand **20** with the large chelate arm ($n = 2$).

New bidentate ligands containing oxazoline and thiocyclohexyl or thiosugar fragments (**22**, **23**) and their 1,3-diphenylallyl Pd(II) complexes were prepared [61]. Since it was not possible to obtain suitable monocrystals, complete ^{1}H and ^{13}C NMR studies were performed. The allyl complexes with ligand **22** or **23** (R = *i*-Pr; R′ = COMe, CO(*t*-Bu)) showed, in solution, the presence of three species. The major species were identified as the *syn-syn-exo* and *syn-syn-endo* isomers in equilibrium at 293 K according to the cross-peaks observed in the NOESY spectra. The *exo* isomer ocurred in greater proportion. At 273 K, the exchange was relatively slow and only NOE effects were observed. An unusual dynamic behavior in the diphenylallyl group was observed.

A group of complexes *fac*-[$ReX(CO)_3$(**NS**)] and *fac*-[$PtXMe_3$(**NS**)] was obtained, where **NS** is a type **17** ligand with the oxazoline in *S* configuration [62]. Detailed NMR studies showed the presence of the four diastereoisomers (Fig. 23a–d) in solution. Above r.t., the epimerization of pairs of diastereoisomers is observed. Atropisomerization occurs after a number of weeks at r.t. and it is assumed that ligand dissociation processes are involved. The X-ray crystal structure of a single isomer of [$ReBr(CO)_3$(**NS**)] (configuration a) showed a bite angle N–Re–S of 78.1°.

Non-linear optical properties were studied in palladium complexes [$PdCl_2$(**NS**)] with type **24** and **25** ligands [63]. Complexation of the palladium ion leads to a net increase in the polarizability of complexes [$PdCl_2$(**25**)].

3.2.2. N,P-donor atoms

The phosphino–oxazoline ligands (**NP**, Chart 5) were developed largely by Pfaltz, Williams and Helmchen for use in several catalytic reactions. The coordination compounds were studied, with some exceptions, in order to discover more about the intermediates of those reactions and to improve selectivity control [4a,64,65].

(Chart 5)

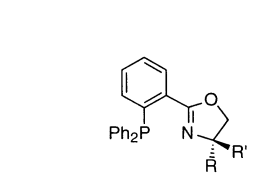

26

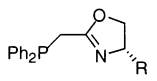

27

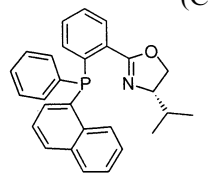

28

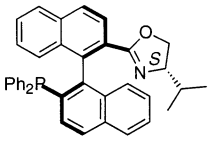

(S, S)

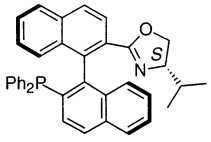

(S, R)

29

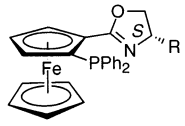

(S, S)

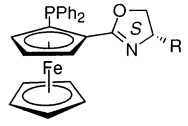

(S, R)

30

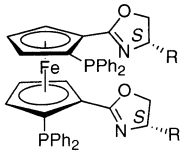

31

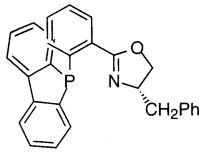

32

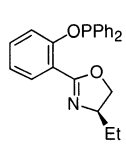

33

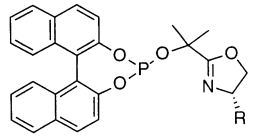

34

Enantioselective Pd-catalyzed allylic substitution is a versatile method for asymmetric synthesis. However, the control of the regioselectivity of nucleophilic attack in non-symmetrical allyl systems remains unresolved. W(0) and W(II) phosphino–oxazoline complexes were prepared in order to investigate this aspect [66]. The ligands used (**26** and **27** with R = *i*-Pr; R′ = H) are able to form five- or six-membered chelate rings respectively. The stability in solution of the complexes containing the five-membered ring is lower than that of those containing the six-membered ring. The crystal structures of the complexes shown in Fig. 24 were determined. Only one diastereoisomer is present in solid state, but in solution the allyl system reaches a broadening maximum at 0°C. Below 0°C, two species become apparent. The signals for the compound with the large chelate ring are still not fully resolved at −60°C in a ratio 5:1 (the major species is assumed to be that of the solid

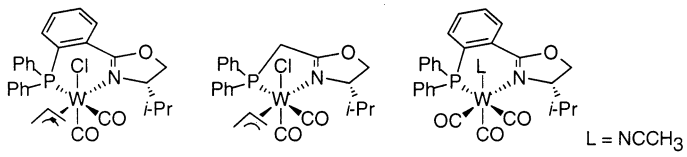

Fig. 24. Five- and six-membered chelate ring tungsten compounds.

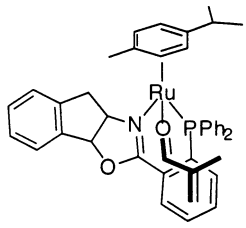

Fig. 25. Proposed intermediate in the Diels–Alder reaction [67].

structure). At −60°C the compound with the five-membered chelate ring shows the major isomer (10:1) with well resolved signals. In solution, at r.t., the ^{31}P NMR spectrum of the complex of W(0) showed two signals (3:1), assigned to the presence of the two diastereoisomers.

The use of chiral (η^6-*p*-cymene)ruthenium complexes as catalysts in enantioselective Diels–Alder reactions further justifies the preparation and determination of the crystal structure of the adduct containing the dienophile methacrolein, using as chiral auxiliar a phosphino–oxazoline ligand. This adduct is assumed to be one of the intermediates of the catalytic reaction (Fig. 25) [67].

A good example of complementary fitting of two homochiral phosphino–oxazoline ligands was reported [68]. The dication $[Ni(\mathbf{NP})_2]^{2+}$ (**26**, R = *i*-Bu, R′ = H) both in solid state and in solution is arranged as shown in Fig. 26. The crystal structure shows that the two **NP** ligands influence each other surprisingly little, due to the complementary nature of the fitting of the two chiral ligands. In solution the ^1H NOESY spectra showed contacts between the methyl groups of the *iso*-butyl fragments and one of the protons of the aryl bridge or one of the diastereotopic methylene protons of the complementary ligand.

Nickel(II) complexes with ten different chiral phosphino–oxazoline ligands **26** and **27** were tested in the Grignard cross-coupling reaction [69], one of which was carefully characterized. The crystal structure of the complex (Fig. 27) showed a distorted tetrahedral Ni(II) center with usual bond lengths or angles. The paramagnetic character (d^8 ion) is clear in solution where different solvent-coordinated species are thought to be present at different temperatures. Surprisingly, the complex with the same ligand $[Ni(\mathbf{NP})_2](OTf)_2 \cdot H_2O$ does not show the same paramagnetic contact-shift in the NMR in solution.

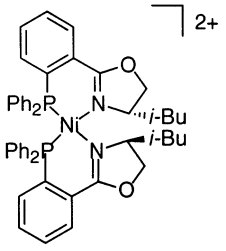

Fig. 26. Structure of the dication $[Ni(\mathbf{26})_2]^{2+}$ R = *i*-Bu, R′ = H.

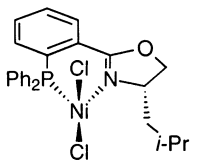

Fig. 27. Pseudotetrahedral structure of the [$NiCl_2$(**26**)] (R = *i*-Pr, R′ = H) compound.

An unexpected dependence of the rate and enantioselectivity on the steric volume of the oxazoline substituent at the stereogenic center was observed: the smaller the substituent, the faster the rate and the higher the enantioselectivity. The solvent also shows an important effect and in THF no enantiomeric excess is observed. Another interesting fact is that the complex containing a **NP** ligand that implies the formation of a five-membered chelate ring did not give any asymmetric induction. The discussion about the preferred geometry of the six-membered chelate ring of the transition metal complexes containing the phosphinoaryl–oxazoline ligand and their effect on the selectivity of the Grignard cross-coupling reaction is included.

A large number of phosphino–oxazolines was tested in the palladium catalyzed allylic alkylations, type **26** and **27** with R = *i*-Pr and R′ = H [70]. In order to discuss the origin of the asymmetric inductions, the cationic allyl intermediates of this reaction have been characterized in solution. At r.t., an 8:1 mixture of the *exo*:*endo* isomers was unambiguously observed (Fig. 28). From NOESY spectra, it is clear that the interconversion between the *exo* and *endo* isomers occurs via the Pd–allyl rotation mechanism. When R = *i*-Pr and R″ = Ph the *exo* isomer was found in the crystal (Fig. 29) [71].

When R = CH_2Ph and R″ = H, the allyl ligand was found to be disordered in the molecular structure [72]. Refining the occupancy factors afforded an *endo*:*exo* ratio of 59:41. But when R = CH_2Ph and R″ = Ph, only the *exo* isomer was present in the solid state. In all three molecular structures, the Pd–C bond to the terminal allylic C-atom *trans* to the P-atom is longer (ca. 0.1 Å) than the bond to the C-atom *trans* to the N-atom. The NMR spectra of the complexes with R = CH_2Ph showed the existence of both isomers *endo*:*exo* in a 1.2:1 and 1:6.5 ratio for the complexes with R″ = H and Ph, respectively. The *exo*-*endo* fluxional process could be observed by NOESY experiments.

In the same study [72], the structure of the zinc complex was reported. The complex shows the expected tetrahedral coordination geometry; and the six-mem-

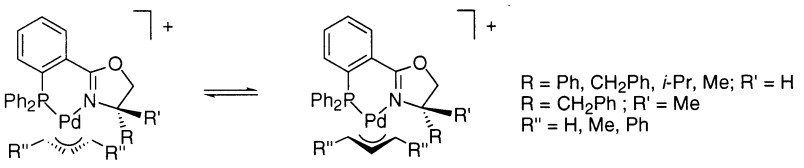

Fig. 28. *Exo*–*endo* equilibrium in the [Pd(allyl)(**26**)]Y complexes.

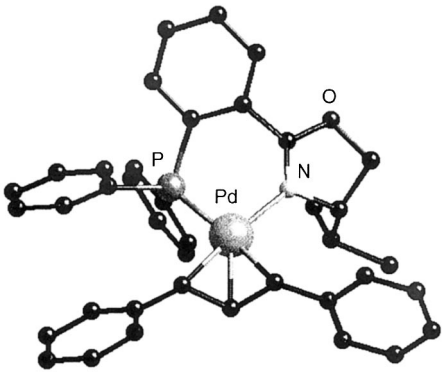

Fig. 29. Molecular structure of [Pd(η^3-1,3-Ph_2–C_3H_3)(**26**)]SbF_6 (R′ = H, R = *i*-Pr). The anion has been omitted for clarity.

bered chelate ring system was analogous to that observed in the square-planar complexes (Fig. 30).

Further analysis of the palladium–allyl complexes was carried out with similar chiral and non-chiral phosphino–oxazoline ligands (**26**). When R″ = Me (Fig. 28), both in solid and in solution *syn-syn* and *syn-anti* configurations of the allyl ligand were observed [73]. To obtain more information about the influence of the counterion on the *endo-exo* equilibria, the hexafluorophosphates and tetrafluoroborates of cations (R = Ph, R′ = H and R″ = H), in enantiomerically pure or racemic form, were studied in solution and in solid state [74].

A discussion on the origin of the asymmetric induction of palladium-catalyzed allylic substitution reactions with mixed **NP** ligands was carried out using new complexes (Fig. 31), fully characterized in solution and in solid state. In this case, *endo* isomers predominate, with consequences for the configuration of the products of the catalytic reactions [75]. New NMR methods have been applied to allyl compounds in order to obtain structural information, when no suitable crystals were obtained [76].

A Pd(0)–olefin complex, one of the intermediates proposed in the allylic substitution catalytic cycle, was recently characterized by ^{1}H NMR spectroscopy. The results obtained were in line with the accepted models for this reaction. The Pd(0)–olefin complex obtained (Fig. 32) is the product of the nucleophilic attack on the allyl carbon *trans* the P-atom [77].

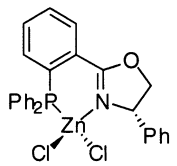

Fig. 30. Tetrahedral structure of the [$ZnCl_2$(**26**)] complex.

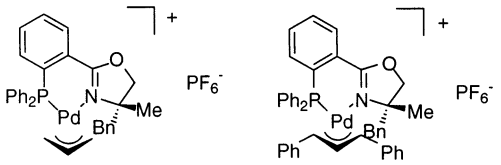

Fig. 31. Allyl–palladium compounds involved in the allylic substitution reaction [75].

The introduction of chirality at the phosphorus atom (**28**) did not improve the enantiomeric excess of allylic alkylation catalytic reactions. The phosphorus atom directed the nucleophilic attack in *trans* position, close to the determinant chiral oxazoline substituent. The crystal structure of the cationic allyl complex contains a disordered mixture of the diastereomeric isomers (Fig. 33). In solution, NOESY and ROESY spectra confirm that the interconversion between the *exo* and *endo* isomers occurs via the $\sigma-\pi$ allyl rearrangement, by opening the Pd–C bond *trans* to the phosphorus atom [71].

Further attempts to improve the asymmetric induction capabilities of the mixed **NP** ligands were reported. It is accepted that the most important factor is the control of the substituent on the C_{sp^3} atom adjacent to the nitrogen atom. Therefore, both sp^3 carbon atoms of the oxazoline moiety were incorporated into a ring (five- or six-membered) in order to increase steric interaction with the allyl ligand in the palladium complex [78].

Other studies of the effect of axial chirality versus central oxazoline chirality with phosphino–oxazoline ligands with binaphtyl skeletons (**29**) have been reported [79,80]. The results indicate that axial chirality is the most influential factor determinant of the stereochemical outcome in the allylic alkylation reaction.

Phosphino–ferrocenyl–oxazoline ligands were used as chiral auxiliaries in several reactions such as Grignard cross-coupling [81], allylic alkylations [82] or hydrosilylation [83]. The isomers **30** were obtained in different proportions 68:32 [84], but further purification led to more than 98% of diasteomeric excess. The complexes synthesized were mainly related to palladium systems, usually by direct reaction between the **NP** ligand and $[PdCl_2(NCCH_3)_2]$.

Two different complexes (from the two isomers of **30** with R = *i*-Pr) were isolated. The two diastereoisomers crystallized and their molecular structures were determined ($[PdCl_2(S,S\text{-}\mathbf{30})]$ (Fig. 34) [84] and ($[PdCl_2(S,R\text{-}\mathbf{30})]$ [81]), showing the six-membered ring formed on complexation with the palladium center folded away from the isopropyl moiety.

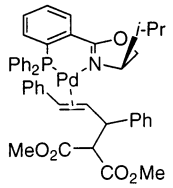

Fig. 32. Olefinic Pd(0) complex, proposed intermediate of the allylic substitution reaction.

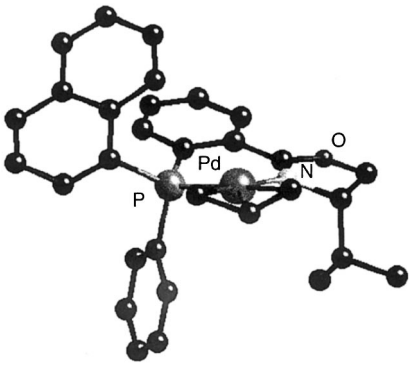

Fig. 33. Molecular structure of $[Pd(\eta^3\text{-}C_3H_5)(\mathbf{28})]SbF_6$. The anion has been omitted for clarity.

The bis(oxazoline)–bis(phosphine)–ferrocenyl ligands were obtained with R = *i*-Pr and *t*-Bu (**31**) in *S* configuration on the carbon close to nitrogen atom of the oxazoline ring. But only the mononuclear $[PdCl_2(S,R\text{-}\mathbf{31})]$ palladium complex was obtained [85]. As shown in the molecular structure (Fig. 35), the coordination takes place on the Cp ring with substituents in *R* configuration. The bite angle N–Pd–P is 91.63°, but the conformation of the six-membered chelate ring of both complexes is very different, as shown in detail in Figs. 34 and 35.

Ruthenium complexes with **30** ligands were prepared and characterized spectroscopically and through the crystal structure determination of the compound $[RuCl_2(PPh_3)(\mathbf{30})]$ when R = Ph [83]. The ruthenium atom has distorted trigonal-bipyramidal geometry with *cis* coordination of the two chlorine atoms, and PPh_3 and one chlorine in axial positions. The complexes were used as catalysts for the asymmetric hydrosilylation of ketones and imines.

The copolymerization of styrene and carbon monoxide using ionic phosphino–oxazoline–palladium complexes (Eq. (13)) produced isotactic or atactic microstructures, depending on the symmetry of the ligand [86]. The initial steps of the reaction could be followed by NMR spectroscopy [87].

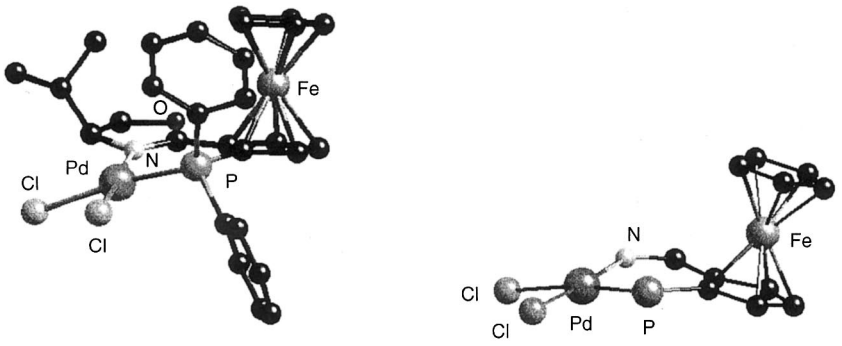

Fig. 34. Molecular structure of $[PdCl_2(S,S\text{-}\mathbf{30})]$ and the detail of the Pd coordination sphere.

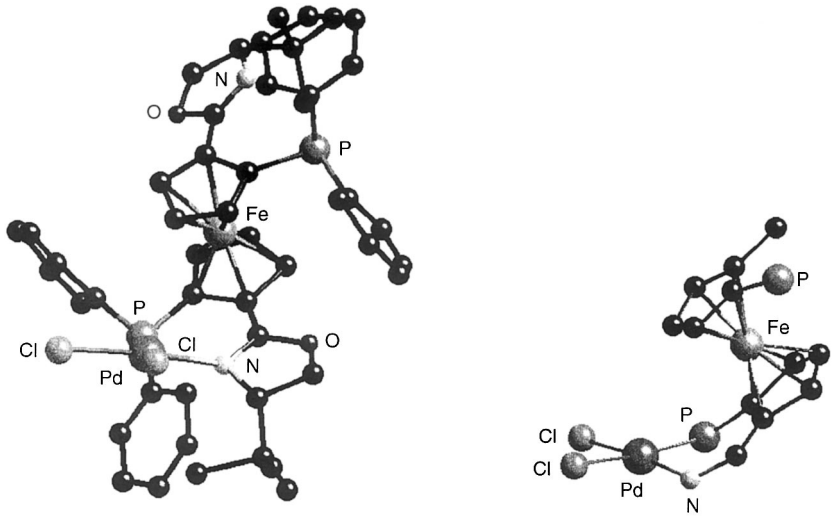

Fig. 35. Molecular structure of $[PdCl_2(S,R\text{-}\mathbf{31})]$ and the detail of the Pd coordination sphere.

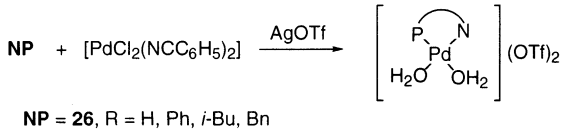

(13)

Phosphinite–oxazoline (**33**) and phosphite–oxazoline (**34**) compounds were also reported. The phosphinite palladium complexes obtained contained a seven-membered chelate ring [45]. The neutral complexes gave very well-defined ^1H NMR signals, but the cationic complexes gave very broad NMR signals even at $-70°C$, showing the *trans*-labilizing ability of the P-atom (Scheme 8).

A good way to develop a method to control the regio- and enantioselectivity of palladium catalyzed allylic alkylations of non-symmetric allyl acetates was proposed by Pfaltz [88]. For this purpose, a new group of **NP** mixed ligands with electron-withdrawing substituents on the phosphorus atom has been prepared,

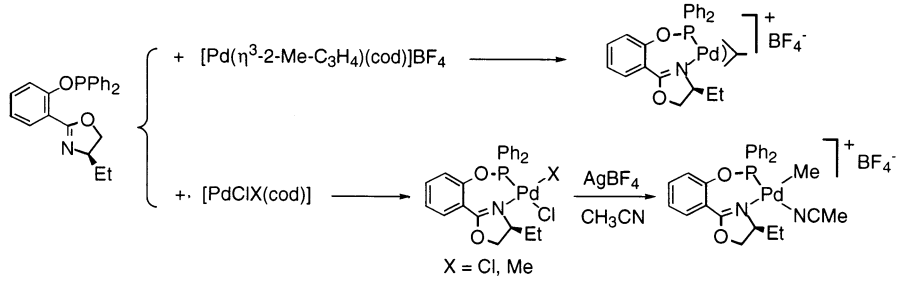

Scheme 8.

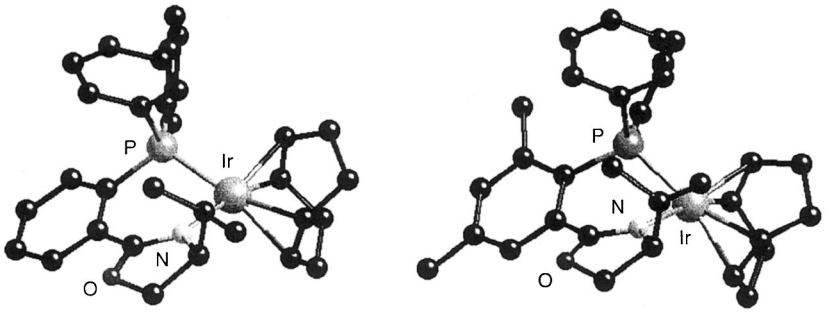

Fig. 36. Molecular structures of [Ir(cod)(**NP**)]PF_6 complexes. The anion has been omitted for clarity.

some of which are phosphite–oxazoline type **34** ligands. The same author used iridium complexes [Ir(cod)(**26**)]PF_6 (R = *i*-Pr, R′ = H) in the enantioselective hydrogenation of imines. The structures of two complexes were determined by X-ray analysis (Fig. 36) [89]. The introduction of a methyl fragment into the phenyl bridge in *ortho* to the phosphorus atom induced the twist of the phenyl group in pseudoequatorial position.

3.3. Bidentate bis(oxazoline) ligands

In the last decade, the C_2-symmetric chiral bis(oxazoline) ligands (**NN**) have received an enormous amount of attention because efficient applications have been found for them in several asymmetric organic processes [3]. Consequently, the characterization of catalytic precursors and intermediate species was studied in order to improve and explain activity and selectivity in these organic transformations. The **NN** ligands that are most frequently studied in the conducting of structural research are shown in Chart 6. They usually coordinate with the metal center by the nitrogen donor atoms in a bidentate fashion, giving chelate rings, from five- to nine-membered cycles. However, some of them also act as bridge ligands, where each nitrogen atom is coordinated to one metal center, stabilizing polymeric complexes [90].

(Chart 6)

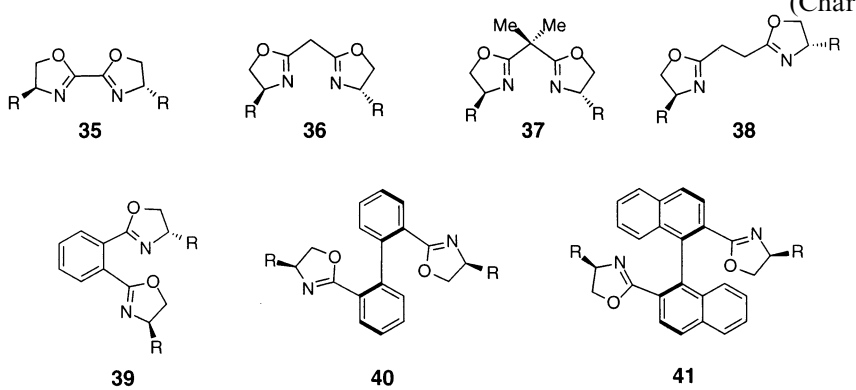

The oxazoline ligands derived from oxalic acid, **35**, stabilize monometallic complexes, with five-membered chelate rings and several metal coordination numbers (Fig. 37): octahedral metal spheres, such as $[Fe(\mathbf{35})_3](ClO_4)_2$ [91] or $[Mo(CO)_4(\mathbf{35})]$ [92]; four metal coordination number, such as $[PdCl_2(\mathbf{35})]$ [93] or $[Cu(\mathbf{35})_2]PF_6$ [94]. Also this kind of ligand acts as a bridge between different metallic centers, as in the formation of inorganic polymers, $[CuBr(\mathbf{35})]_n$ and $[Cu_2I_2(\mathbf{35})]_n$ [90b]. In general, **35** ligands stabilize relatively low metal oxidation states. Therefore, Fe(III) complexes, analogous to the previously described $[Fe(\mathbf{35})_3]^{3+}$, could not be isolated [91]. This suggests a considerable ligand π-acceptor contribution. This bonding feature was experimentally revealed by the work of Merlic et al. on the correlation between the ^{95}Mo chemical shift and the ligand π-acceptor ability in a similar series of complexes, $[Mo(CO)_nL_{6-n}]$, where L was a nitrogen-based ligand [92]. They found that a decrease in ligand π-acceptor ability (isonitrile > bis(oxazoline) > diimine > diamine) corresponded to high-frequency shifts in the ^{95}Mo NMR spectra. Then, ligands **35** have higher π-acceptor behavior than diimines [95]. This trend should also be revealed by analysis of structures in the solid state. Unfortunately, to date, no X-ray structures containing chelate **35** have been determined.

Ligands **36** and **37** give six-membered anionic or neutral chelate complexes. The neutral or ionic nature of the oxazoline fragment is due to the Brønsted basicity of the methylene bridge group. Bis(oxazolines) **36** can act as anionic (by deprotonation of the CH_2 bridge unit) or neutral ligands, whereas **37** (with disubstituted methylene bridge, CR'_2) is only able to coordinate as a neutral ligand. The neutral or anionic behavior of **36**, reported in the literature, depends on the starting precursors used in the synthesis of the complexes (Scheme 9) [96–98].

In addition, neutral **36** and **37** ligands differ in their Lewis basicity. The structural study carried out by Woodward et al. with tungsten complexes,

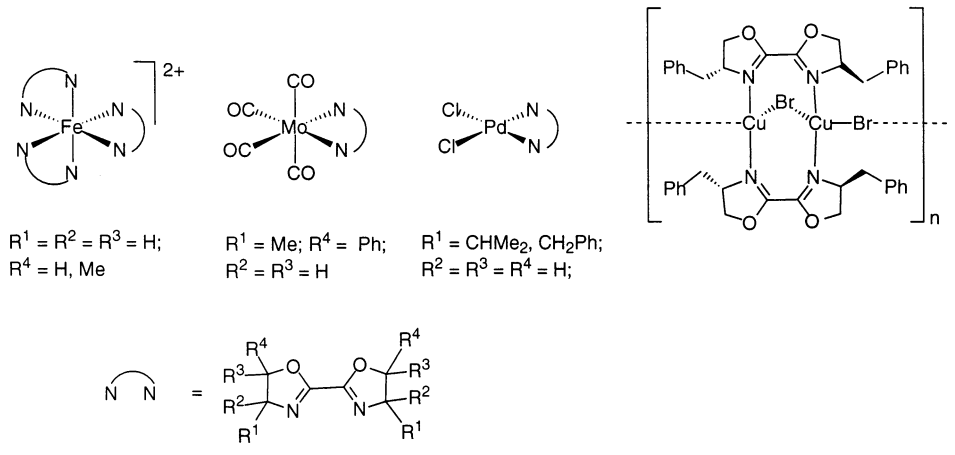

Fig. 37. Coordination behavior of ligands **35**.

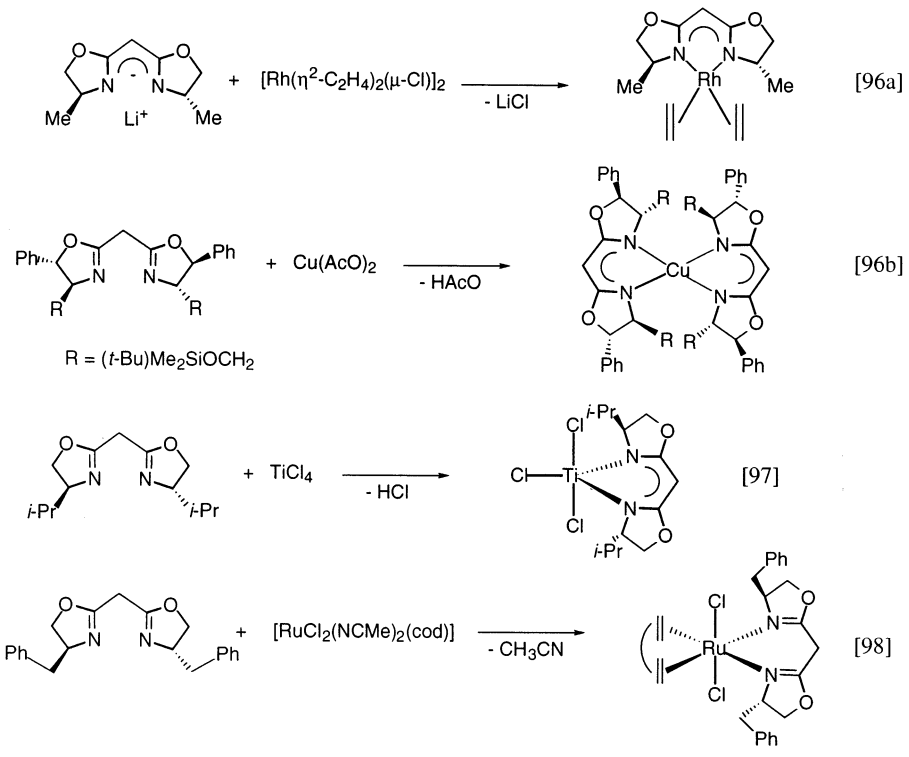

Scheme 9.

$[W(CO)_4(\mathbf{36})]$ and $[W(CO)_4(\mathbf{37})]$ (**36** and **37**, R = *i*-Pr, Fig. 38), proves that **37** are stronger σ donor ligands than are analogous **36** [98]. Therefore, W–N bond lengths for complex $[W(CO)_4(\mathbf{37})]$ (2.187, 2.192 Å) are shorter than those in $[W(CO)_4(\mathbf{36})]$ (2.261, 2.256 Å). Besides, the CMe_2 bridge group between the two oxazoline moieties results in deformation from an essentially planar ring for $[W(CO)_4(\mathbf{36})]$ to an envelope conformation for $[W(CO)_4(\mathbf{37})]$.

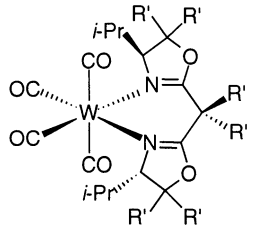

36, R' = H
37, R' = Me

Fig. 38. Structure of the $[W(CO)_4L]$ L = **36**, **37** complexes.

The anionic electron-rich ligands **36** are able to stabilize high-metal oxidation states, because they can act as σ- and π-electron donors, analogously to semicorrin ligands [99] but unlike the neutral oxazolines, weaker electron-donors and even π-acceptors [92]. Therefore, high yields of titanium(IV) complexes were prepared [97]. For these complexes, a chelate coordination of the ligand is proposed on the basis of infrared data (the imine stretching, ν(C=N), is shifted at lower frequencies relative to the free ligands) and NMR spectra (^{1}H and ^{13}C downfield shifts), giving pentacoordinate compounds (Scheme 9).

Complexes containing chelating **37** ligands, with four- and six-coordination numbers for the metal atom, were fully characterized, both in solid state and in solution. Among four-coordination numbers, structures with square-planar (Pd) and tetrahedral (Cu, Zn) metal geometry were analyzed by X-ray diffraction.

To date, the most important structural studies of palladium complexes have been concerned with allyl derivatives, due to their success as catalytic species in asymmetric allylic substitutions [41]. It is because of these homogenous catalytic applications, that NMR studies have been vital in proving the specific nucleophilic attacks. With this in mind, Pfaltz and co-workers prepared the complexes [Pd(η^3-C_3H_5)(**37**)]PF_6 and [Pd(η^3-1,3-Ph_2–C_3H_3)(**37**)]PF_6 (Eq. (14)) [100].

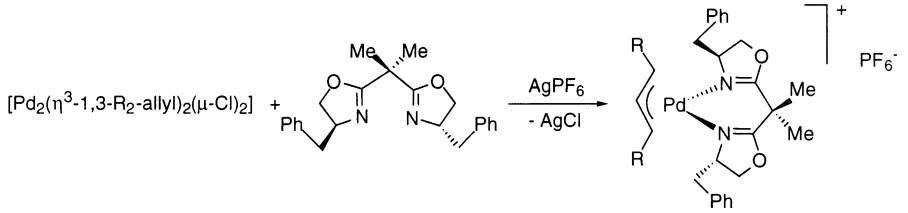

(14)

Analogous allyl compounds formed with other chelating *N*-based ligands enabled fine structures in the interactions between the nitrogen-ligand fragment and the allyl group [101] to be studied, since the *N*-moiety was rigid enough to have a fixed conformation. Unlike the so-called 'reporter' ligands, the bis(oxazoline) in [Pd(η^3-C_3H_5)(**37**)]PF_6 and [Pd(η^3-1,3-Ph_2–C_3H_3)(**37**)]PF_6 cannot be considered a rigid group. So, NMR spectra (NOE experiments) suggest that complex [Pd(η^3-1,3-Ph_2–C_3H_3)(**37**)]PF_6 (**37**, R = CH_2Ph) exists in two isomers, which mutually interconvert on the NMR time scale. These isomers result from the boat-like conformation of the chelate cycle, which is also observed in solid state. The crystal structure shows that one of the two bond lengths of Pd–C (allylic terminal atoms) is longer (ca. 0.05 Å) than the other, unlike [Pd(η^3-C_3H_5)(**37**)]PF_6 (Fig. 39). In addition, the ligand in this latter complex adopts an almost planar arrangement, but in [Pd(η^3-1,3-Ph_2–C_3H_3)(**37**)]PF_6 it is strongly distorted from planarity due to the steric repulsion between the phenyl allylic group and the benzyl substituent of the ligand [102]. This distorsion might explain the difference in nucleophility of both terminal allyl carbons.

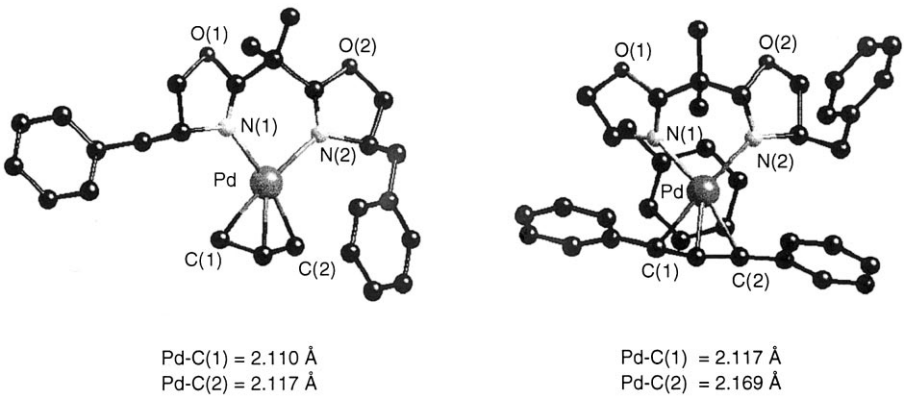

Fig. 39. Molecular structures of $[Pd(\eta^3\text{-}C_3H_5)(\mathbf{37})]PF_6$ and $[Pd(\eta^3\text{-}1,3\text{-}Ph_2\text{–}C_3H_3)(\mathbf{37})]PF_6$(R = Ph). The hexafluorophosphate anions have been omitted for clarity.

Asymmetric allylic fragments were also employed in the synthesis of complexes (Fig. 40) [103]. In this case, four isomers are possible, depending on the *syn*/*anti* position of the allylic substitution and the relative position between this substituent and the group on the sterocenter of the oxazoline. The NMR research showed the isomeric distribution for each complex. In general, the major diastereromer is the less crowded *syn* complex and stereoselectivity increases in the sequence of the R′ size: phenyl < 1-naphtyl < $COSiMe_2Ph$.

NMR studies of acyl compounds at low temperatures showed that bis(oxazolines) can also coordinate, at least in solution, as monodentate ligands (Eq. (15)) [104].

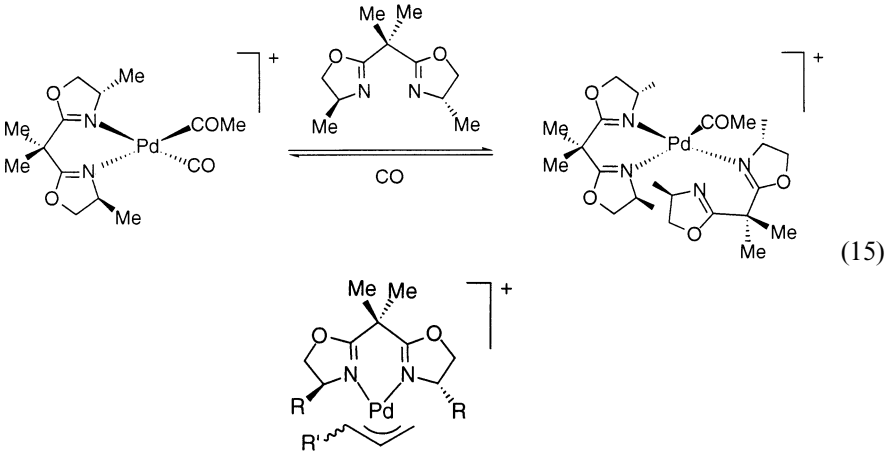

(15)

Fig. 40. Palladium complexes containing unsymmetrical allyl groups.

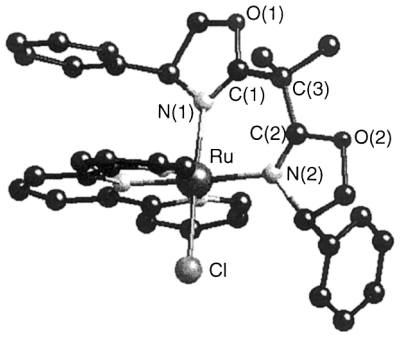

Fig. 41. Molecular structure of $[RuCl(trp)(\mathbf{37})]BF_4$ (R = Ph). The tetrafluoroborate anion has been omitted for clarity.

Evans and co-workers were able to rationalize the superior activity of Cu–bis(oxazoline)-based catalysts compared to other cationic Lewis acid metal systems, by studying crystal structures of complexes and computer-generated structures of intermediates [105].

The X-ray structures of copper complexes, $[CuCl_2(\mathbf{37})]$ and $[Cu(H_2O)_2(\mathbf{37})](SbF_6)_2$ (**37**, R = *t*-Bu, Eq. (16)), exhibited a distorted square-planar arrangement around the metal atom, with the coordinated chloro or aqua ligands displaced 33–37° out of the Cu–bis(oxazoline) plane. This structural feature enabled organic dienophiles, in Diels–Alder reactions, to coordinate with the catalytic precursor in a chelating manner, giving high enantioselection in the process.

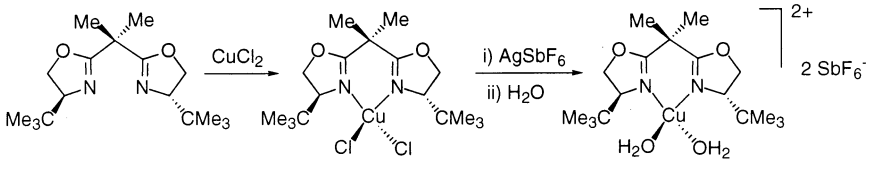

(16)

Tetrahedral zinc complexes were also analyzed by X-ray diffraction: $[ZnCl_2(\mathbf{37})]$, analogous to the chloro–copper complex described above (Eq. (16)) [105a] and $[ZnCl_2(\mathbf{38})]$ (**38**, R = *t*-Bu), which is the best Lewis acid catalyst for the Diels–Alder of *N*-crotonyloxazolidinone with cyclopentadiene [106].

The first structure involving a neutral bis(oxazoline) ligand bonded to a six-coordinate ruthenium atom was reported by Takeuchi and co-workers in 1995, $[RuCl(trp)(\mathbf{37})]BF_4$ (trp = terpyridine; **37**, R = Ph) [107] (Fig. 41). Previously only a few examples with tungsten and ruthenium complexes had been described [66,98]. The ruthenium atom has a distorted octahedral environment (for example, N(1)–Ru–N(2) = 84.1°), with a *mer* terpyridine ligand, a *cis* bis(oxazoline) group and a chloride anion. The bond lengths Ru–N(1) and Ru–N(2) (2.094 and 2.124 Å, respectively) confirmed the greater *trans* influence of the nitrogen atom compared to

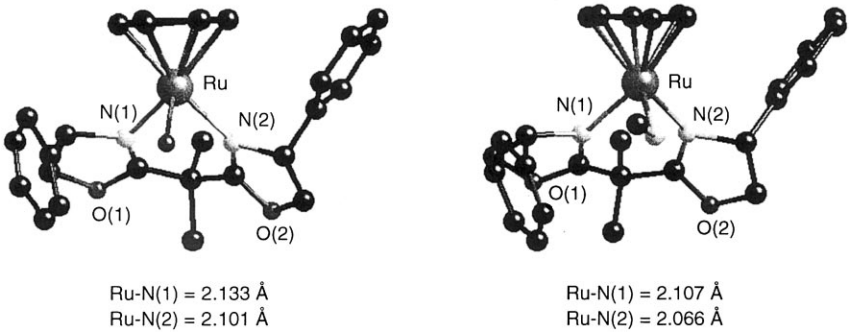

Fig. 42. Molecular structures of $[Ru(\eta^6\text{-}C_6H_6)(H_2O)(\mathbf{37})](BF_4)_2$ and $[Ru(\eta^6\text{-}C_6H_6)(NH_2Me)(\mathbf{37})](BF_4)_2$ (R = Ph). The tetrafluoroborate anions have omitted for clarity.

that of the chlorine atom. The NMR analysis revealed that the chiral bis(oxazoline) ligand loses C_2 symmetry upon coordination, as in most structures with C_2 symmetrical ligands. It is also important to note the upfield shift of a phenyl proton of the oxazoline moiety (ca. 3 ppm relative to the uncoordinated ligand) because it is directed into the center of an aromatic ring of terpyridine, as the crystal structure reveals.

More recently, organometallic half-sandwich Ru and Rh complexes have been prepared using bis(oxazoline) ligands, **37** and **39** [33,108]. With **37**, structural studies showed the loss of C_2 symmetry upon coordination, both in solution and in solid state. The NMR spectrum of $[Ru(\eta^6\text{-}C_6H_6)(H_2O)(\mathbf{37})](BF_4)_2$ (**37**, R = Ph) at r.t. was consistent with a C_2 symmetric structure (with only one resonance for each different hydrogen oxazoline atom being observed), but the patterns split at lower temperatures. These NMR features are consistent with a rapid interconversion between two conformations. In contrast to the aqua complex, the amine complexes, $[Ru(\eta^6\text{-}C_6H_6)(L)(\mathbf{37})](BF_4)_2$ (where $L = NH_2Me$, NH_3, $NH_2(n\text{-Bu})$), are rigid in solution on the NMR time scale [108].

The X-ray structures of ruthenium complexes (Fig. 42) and $[RhCl(\eta^5\text{-}C_5Me_5)(\mathbf{37})]SbF_6$ (Fig. 43) (**37**, R = *i*-Pr) show that in each case, the metal atom has pseudo-octahedral geometry, with $\eta^6\text{-}C_6H_6$ (Ru compounds) and the $\eta^5\text{-}C_5Me_5$ (Rh complex) group occupying three *fac* coordination sites. For the three structures, the $M-N_{oxazoline}$ bond lengths differ, with the greatest difference being that of the rhodium complex (Rh–N(1) = 2.117; Rh–N(2) = 2.157 Å). This asymmetry can be

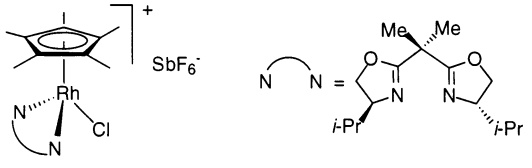

Fig. 43. Pseudotetrahedral structure of the $[RhCl(\eta^5\text{-}C_5Me_5)(\mathbf{37})]SbF_6$ complex.

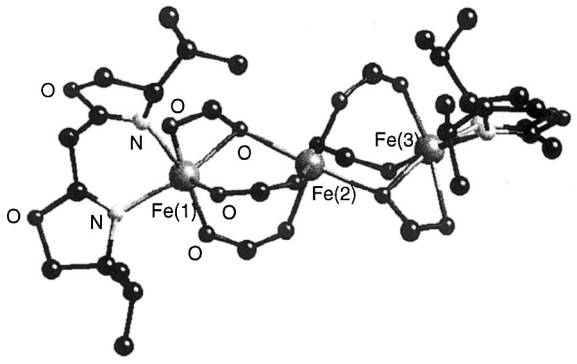

Fig. 44. Molecular structure of $[Fe_3(O_2CPh)_6(\mathbf{36})_2]$ (R = *i*-Pr). The carboxylate phenyl groups have been omitted for clarity.

explained by the steric repulsion between the substituent on one of the oxazoline fragments and the arene group, which has greater effects for the isopropyl than the phenyl fragment.

However, heavy transition metals are not the only complexes to show six-coordination. First row metals can also give this kind of coordination with bis(oxazoline) ligands. Therefore, Lippard and co-workers described a trimeric iron complex, $[Fe_3(O_2CPh)_6(\mathbf{36})_2]$ (**36**, R = *i*-Pr), where each metal atom has a hexacoordinate arrangement and the two terminal iron atoms are bonded to a neutral chelate bis(oxazoline) and two carboxylate bridges (Fig. 44) [109].

Bis(oxazolines) derived from malonic acid (**36**, **37**) can also act as bridges between two metal atoms. Therefore, $[Cu(\mathbf{37})]_n(OTf)_n$ (**37**, R = *t*-Bu) is a single-stranded helical polymer (Fig. 45) [90a]. The bis(oxazoline) occupies a bridging position between two nearly linear copper atoms, each of which is coordinated with two nitrogen atoms. The triflate anion is dissociated from the metal. This structure

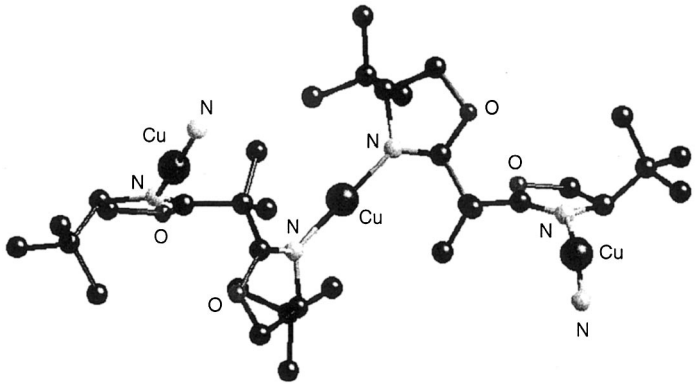

Fig. 45. Molecular structure of $[Cu(\mathbf{37})]_n(OTf)_n$ (R = *t*-Bu). The triflate anions have been omitted for clarity.

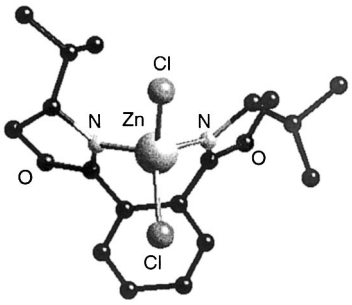

Fig. 46. Molecular structure of [$ZnCl_2$(**39**)] (R = *i*-Pr).

reflects the ability of bidentate ligands to enforce macromolecular organization. In this particular case, the ligand, due to its own chirality, directs both the assembly of the polymer and the sense of helicity.

Tethered aromatic groups between the two oxazoline moieties introduce new structural aspects into the discussion. In the literature, monometallic complexes with **39–41** have been reported. These bidentate ligands coordinate with metal atoms, giving rigid seven- or nine-membered cycles, with bite angles (N–M–N) that can be greater than those shown by the ligands described above. These structural features explain the differences in stability of complexes using similar ligands. Therefore, Cu(I) complexes with **37**, [Cu(OTf)(**37**)] (OTf = triflate anion; **37**, R = Ph, *t*-Bu or *o*-Tol), are stable in solid state but decompose in solution [110], whereas [Cu(OTf)(**40**)] (**40**, R = *t*-Bu) is stable in air either in the solid state or in solution [111]. Also, the structural differences between **39** and biphenyl and binaphthyl derivatives should be noted. With regard to chirality, **40** and **41** give typical examples of atropoisomerism due to their restricted rotation around the axis between the two aromatic fragments.

Tetrahedral and square-planar complexes containing **39** ligands have been characterized. Bolm and co-workers prepared a series of Zn compounds, [$ZnCl_2$(**39**)], with different substituents on the C_{sp^3} adjacent to oxazoline nitrogen (Eq. (17)) [112].

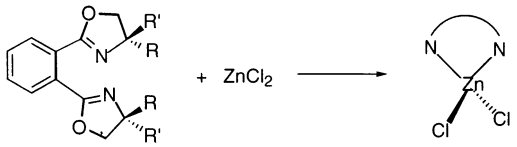

R = *i*-Pr, CHMeEt, Ph, Bn; R' = H
R = R' = Me (17)

The molecular structure of one of these complexes (R = *i*-Pr, R′ = H) showed that the geometry around the zinc atom is tetrahedral, bonded to the chelate bis(oxazoline) and two chlorine atoms. As shown in Fig. 46, one of the isopropyl groups points into the metallic cycle, whereas the other one points out, causing a

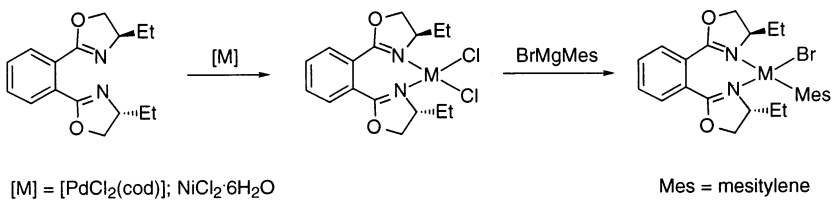

Scheme 10.

non-equivalence of the two substituents. The seven-membered cycle is not planar, with the dihedral angles between oxazoline moieties and phenyl bridge ca. 46.6°. In solution at r.t., the ^{1}H NMR is consistent with a C_2 symmetric structure (presumably time-averaged), but at lower temperatures, loss of symmetry can be observed.

Recently, square-planar palladium and nickel complexes were synthesized in our laboratory (Scheme 10) [113]. NMR studies at variable temperature showed that the two oxazoline fragments, unlike the zinc compounds described above, are non-equivalent in the whole temperature range. This can be explained by the restricted rotation around the single bonds C_{aryl}–$C_{oxazoline}$ because of the coordination of nitrogen atoms at the metal center. So, efficient bidentate coordination towards a single metal atom in the (*aR*, *aR*) or (*aS*, *aS*) isomers is not possible due to the highly strained ring [114]. Therefore, only the (*aR*, *aS*) isomer can stabilize the non-planar seven-membered ring. The X-ray diffraction determination of [$PdCl_2$(**39**)] (**39**, R = Et) also proved that the C_2 axis does not exist in the solid state and shows two non-equivalent oxazoline moieties and therefore, two non-equivalent chloro positions (Fig. 47). The bite angle N–Pd–N is 85.8° and each oxazoline ring and the phenyl bridge are tilted.

The non-equivalence of chlorine atoms was also confirmed by the ^{1}H NMR spectra of [MBr(mesitylene)(**39**)] (M = Ni, Pd; **39**, R = Et), due to the formation of two isomers (ratio 2:1), depending on the halogen position substituted by the organic group. The non-statistical ratio reflects the larger steric hindrance between the ethyl–oxazoline and mesitylene groups.

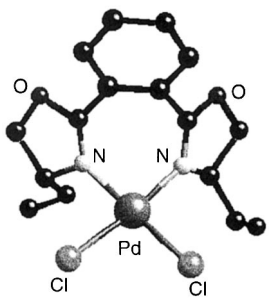

Fig. 47. Molecular structure of [$PdCl_2$(**39**)] (R = Et).

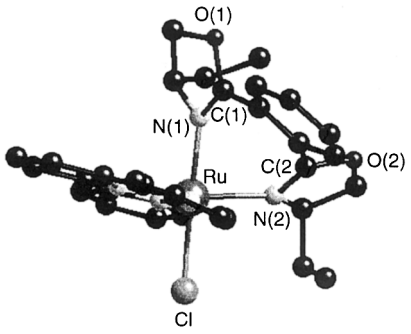

Fig. 48. Molecular structure of [RuCl(trp)(**39**)](PF_6) (R = Et). The hexafluorophosphate anion has been omitted for clarity.

We also prepared ruthenium complexes with **39** (R = ethyl) [115]. Analogous to [RuCl(trp)(**37**)]BF_4 (Fig. 41), the ruthenium shows a distorted octahedral environment with the terpyridine and one nitrogen oxazoline atom in the equatorial plane, and the other nitrogen oxazoline and chlorine atoms in axial positions (Fig. 48). The bite angle N(1)–Ru–N(2) is 82.4°. However, for this structure both oxazoline fragments are twisted at greater angles away from each other: the dihedral angles between each oxazoline and the phenyl bridge group are 32.7 and 43.9°, whereas for [RuCl(trp)(**37**)]BF_4 the dihedral angles Ru–N(1)–C(1)–C(3) and Ru–N(2)–C(2)–C(3) are 6.9 and 12.4°.

In 1995, Corey and co-workers published the first structure of Cu(I) with a biphenyl derivative (**40**), [Cu(OTf)(**40**)] (**40**, R = *t*-Bu), with four *ortho* substituents, two methyl and two oxazoline units [111]. As shown in Fig. 49, the copper atom is tricoordinate, bonded to the two nitrogen atoms of the *N*-ligand and the oxygen of triflate anion, giving a nine-membered chelate ring. The bite angle N–Cu–N is 134°, the highest value for structures containing chelate bis(oxazolines), while the two phenyl rings are nearly perpendicular.

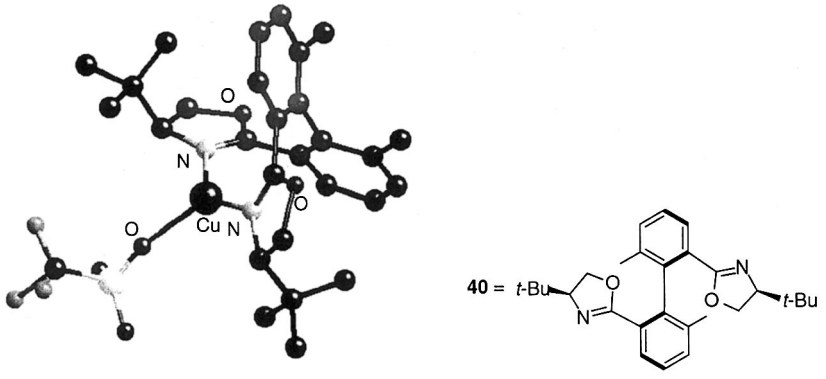

Fig. 49. Molecular structure of [Cu(OTf)(**40**)].

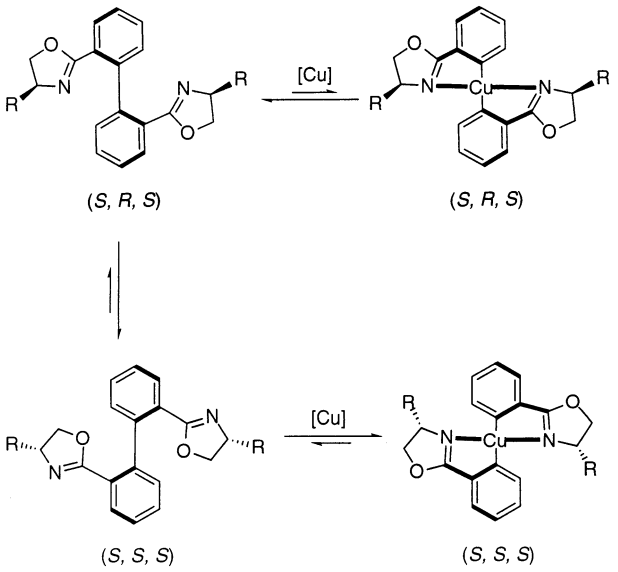

(R = *i*-Pr, *t*-Bu)

Scheme 11.

More recently, Ikeda and co-workers examined the complexation in solution of Cu(I) precursors (such as $[Cu(OTf)(C_6H_6)_{0.5}]$) with **40** [116]. For ligands with only two *ortho* substituents (Scheme 11), only one isomer is formed. Analysis of CPK models indicates that the complex is probably the (*S*, *S*, *S*) isomer because the steric repulsions are smaller than for the (*S*, *R*, *S*) isomer (where the first and last label show the absolute configuration of the oxazoline sterocenters and the label in the middle refers to the axial configuration).

Uozumi et al. have described the first structure with ligand **41**, $[Pd(CO_2CF_3)_2(\mathbf{41})]$ (**41**, R = *i*-Pr) (Eq. (18)) [117].

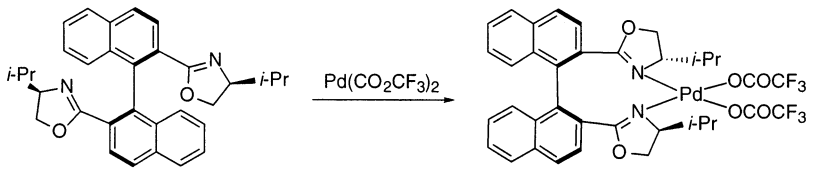

(18)

The geometry around the palladium is distorted square-planar in which two nitrogen atoms of the bidentate ligand and two oxygen atoms of the trifluoroacetate anions are bonded to the metal center. The bite angle N–Pd–N is 100.3° with the two naphthyl groups in perpendicular positions. This conformation leads to the isopropyl substituents on the oxazoline fragments being perpendicular to the coordination plane. This structural feature is also observed in solution. In the ^1H NMR spectrum, a high-field chemical shift (-0.01 ppm) is observed, due to an isopropyl methyl group lying near to the naphthyl ring.

Other C_2 symmetric **NN** ligands (Chart 7) were synthesized and applied in a range of catalytic homogenous processes, including dendritic systems [118f,g], but, to date, no coordination studies have been reported.

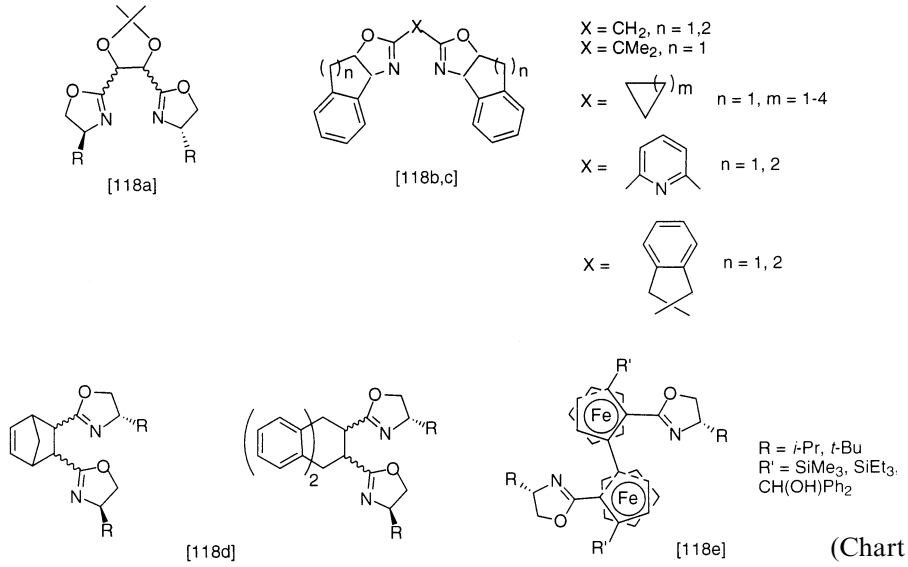

(Chart 7)

3.4. Polydentate oxazoline ligands

'Pybox' is the widely accepted name of the 2,6-(bisoxazolin-2-yl)pyridine ligands (**42**, Chart 8), the use of which is also related to organic synthesis reactions. The complexes are mainly hexacoordinate (Ru, Rh, Mo, W, Re) or tetracoordinate (Pd, Cu).

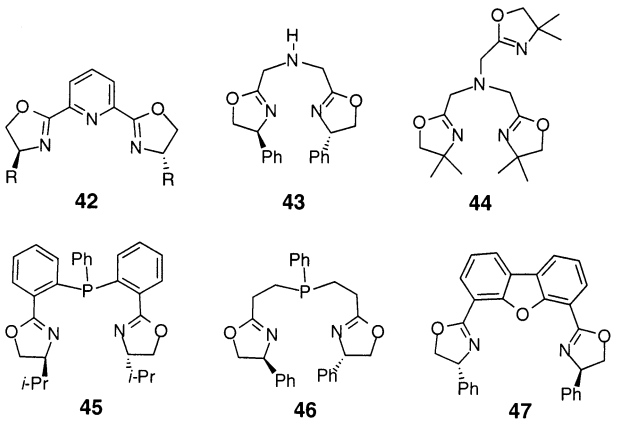

(Chart 8)

Fig. 50. Carbene complexes with **42** ligands.

Neutral and ionic ruthenium complexes *trans*-[$RuCl_2$(**42**)(py)], and *cis*- and *trans*-[RuCl(**42**)$(py)_2$]PF_6 (R = *i*-Pr) are fully characterized in solid state and in solution [119]. Cyclic voltammetry studies in both [Ru(**42**)$(py)_2(H_2O)$]$(PF_6)_2$ and [Ru(**42**)(bipy)(H_2O)]$(PF_6)_2$ (R = *i*-Pr) suggest single, reversible, two-electron oxidation coupled with a two-proton transfer, giving [Ru(O)(**42**)$(py)_2$]$(PF_6)_2$ and [Ru(O)(**42**)(bipy)]$(PF_6)_2$ tested in oxygen transfer reactions.

The preparation of carbene compounds, proposed intermediates of the cyclopropanation reaction in which pybox ligands are efficient, was achieved by Nishiyama's group [120,121] (Fig. 50).

The pybox ligand with bulky isopropyl substituents may be necessary to stabilize the carbene complex since, when bis(oxazolinyl)pyridine was used, the analogous carbene complex could not be obtained. The molecular structure of one ruthenium–carbene complex was determined [122]. The carbene ligand is perpendicular to the pybox equatorial plane (Fig. 51).

Olefin complexes of ruthenium and osmium with pybox are useful starting materials. The molecular structure in solid state of the ruthenium ethylene complex shows that ethylene lies in the same plane as the pybox ligand (Fig. 52) [123,124]. Other dichloro–ruthenium complexes containing a group of prochiral olefins were studied (Fig. 53). The NMR spectrum and the crystal structure determination of the complex with acrolein confirm the presence of η^2-olefin complexes in single conformation, thus demonstrating their ability to discriminate between the enantiofaces of the olefin, and also fix the conformation of the substituents [125].

The neutral Ru(II) complex containing one molecule of carbon monoxide was obtained (Fig. 53), and no further substitution by CO was observed [124b]. The

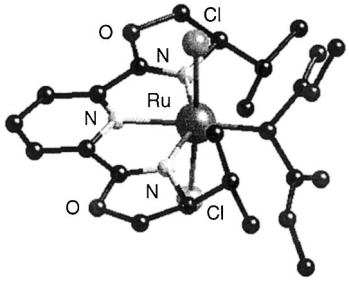

Fig. 51. Molecular structure of [$RuCl_2$(**42**)$(C(CO_2Me)_2)$] (R = *i*-Pr).

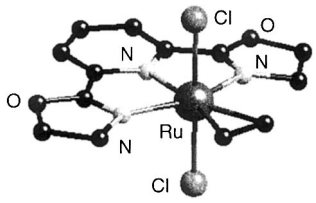

Fig. 52. Molecular structure of $[RuCl_2(\eta^2\text{-}C_2H_4)(\mathbf{42})]$ (R = H).

diacetate carbonyl, the dichloro ethylene and the dichloro pyridine complexes show $Ru-N_{py}$ distances of 2.073, 2.004 and 1.945 Å respectively, according to the *trans*-influence and rigidity of the pybox ligand.

Rhodium compounds were obtained and the crystal structure of the isopropyl derivative determined $[RhCl_3(\mathbf{42})]$ (Fig. 54). The complexes are active in the hydrosilylation of ketones when silver salts are added [126,127].

Complexes in low oxidation states of molybdenum, tungsten, rhenium [122,123] and Pt(IV) [123] contain the pybox ligand in a bidentate fashion. In solution these complexes undergo a fluxional process that exchanges the coordinate and the pendant oxazoline groups. The different exchange pathways, 'tick–tock twist' and 'rotation', are discussed mainly in rhenium and platinum complexes. The molecular structure of *cis*-$[Mo(CO)_4(\mathbf{42})]$ (**42**, R = *i*-Pr) [128] and the *fac*-$[ReCl(CO)_3(\mathbf{42})]$ (**42**, R = Me) (Fig. 55) [129] are determined.

Copper(II) complexes with pybox ligands form useful chiral Lewis acids in reactions such as enantioselective Diels–Alder [130,131] or aldol additions [131–133], but other reactions have also been tested [134,135]. The nature of the intermediates of the aldol reaction has been discussed, and a square-pyramidal coordination supported by EPR spectroscopy proposed [132].

Palladium compounds containing pybox ligands in tetracoordinate environments were well characterized [136,137]. Interesting results from X-ray structural studies comparing $[Pd(CH_3CN)_2(bipy)](BF_4)_2$ and $[Pd(CH_3CN)(\mathbf{42})](BF_4)_2$ (**42**, R = *i*-Pr) showed similar bite angles of the five-membered ring of the complexes (80.9° for the bipy complex, and 79.5 and 81.8° for the pybox one) [136]. So the inherent difference caused by ring size, five-membered or six-membered in the oxazoline or bipy ligands, is reflected only in the bond lengths $Pd-N_{bipy} = 1.992$ and 2.004 Å or in the pybox complex Pd–N(2) = 1.922 Å, Pd–N(1) = 2.017 and Pd–N(3) = 2.030

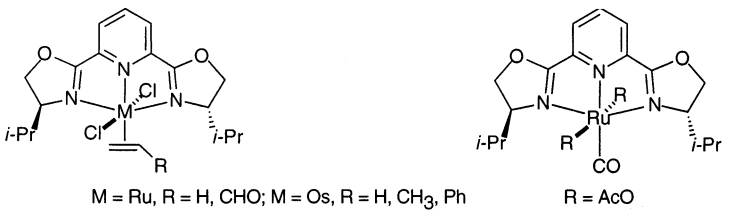

Fig. 53. Ru and Os complexes containing olefins or CO ligands.

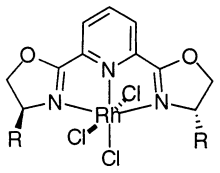

Fig. 54. Rhodium precursors in the hydrosilylation on ketones.

Å (with N(1) and N(3) being from the oxazoline, and N(2) from the pyridine fragment).

Several complexes containing chiral pybox ligands with different substituents (R = *i*-Pr, Ph, Bn, *p*-$EtOC_6H_4$) have been obtained and some of them structurally characterized (Fig. 56), but in terms of the reactivity it must be noted that the pybox ligand is completely substituted by isonitriles. So isonitriles seem to lead to ineffective results in enantioselective organic synthesis, whether they are reactive or solvent [137].

Pybox ligands also appear in polynuclear complexes in unusual coordination modes. Compound **42** with R = benzyl or R = phenyl gave silver binuclear $[Ag_2(\mathbf{42})_2](BF_4)_2$ or trinuclear $[Ag_3(\mathbf{42})_3](BF_4)_3$ species containing two or three pybox molecules (Fig. 57) [138]. The different organization of the compounds is discussed in terms of the staking interaction in the trinuclear complex. The crystal structures show small interactions between the N atom of the pyridine units and the silver atom: for binuclear compounds the average bond distance Ag–N(2) = 2.82 Å, while for the trinuclear complex two different bond distances are observed: 2.65 and 2.82 Å. The distances with the N atoms of the oxazoline moieties are about 2.15 Å.

The **NN′N** (**43**) ligand was prepared for use in the Ru-catalyzed asymmetric transfer hydrogenation of ketones [139]. In the process, one molecule of PPh_3 had to be coordinated to the complex. The N–H proton also seems to play an important but unknown role in the reaction.

The tripodal tris(oxazoline) ligand **44** was used to prepare copper(I) complexes and an unexpected binuclear compound with distorted trigonal-planar coordination around the copper atom was obtained. The bond distances Cu–N(1), Cu–N(2), Cu–N(3) and Cu–N(4) are 2.122, 1.948, 1.957 and 2.735 Å, respectively [140] (Fig. 58).

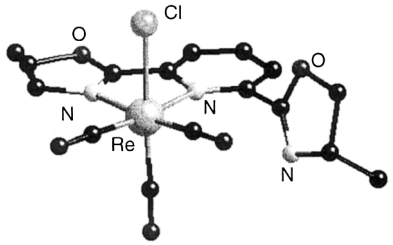

Fig. 55. Molecular structure of *fac*-[$ReCl(CO)_3$(**42**)] (R = Me).

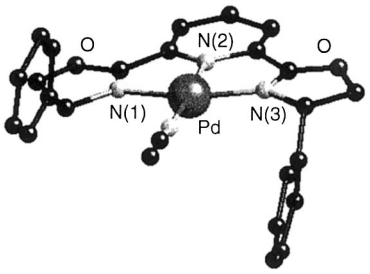

Fig. 56. Molecular structure of $[Pd(CH_3CN)(\mathbf{42})][BF_4]_2$ (R = Ph). The tetrafluoroborate anions have been omitted for clarity.

The preparation of **NPN** (**45**, **46**) ligands was achieved by direct attack of the fragment containing the oxazoline group on $PPhCl_2$ or by addition of acrylonitrile to $PPhH_2$ and then closure of the oxazoline ring with aminoalcohol. Mixtures of these ligands and $[RuCl_2(C_6H_6)_2]$ were used in the asymmetric transfer hydrogenation of ketones [141].

The **NON** (**47**) ligand gives transition metal(II) perchlorates of Fe, Co, Ni, Cu, and Zn [142,143]. The X-ray structure of $[Ni(\mathbf{47})(H_2O)_3](ClO_4)_2$ shows a C_2-symmetric *trans*-chelating ligand with an almost linear N–Ni–N angle of 174.2° (15–20° greater than the angles observed in the pybox analogous complexes) and the Ni–N distances of 2.059 and 2.065 Å (Fig. 59). These compounds are interesting because of their excellent catalytic activity and enantioselectivity in the Diels–Alder reaction.

The synthesis of cyclic ligand-containing peptides enabled their ability to coordinate with a wide group of metal ions to be studied, where each cyclopeptide contains three 4,5-dihydroxazole units (Fig. 60). Only weak interactions were observed except with silver ions. In the latter case, an Ag_4 cluster stabilized by two

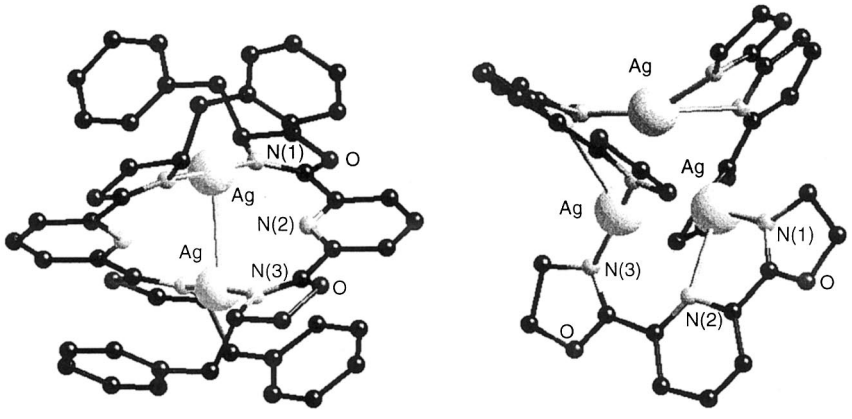

Fig. 57. Molecular structure of $[Ag_2(\mathbf{42})_2](BF_4)_2$ and $[Ag_3(\mathbf{42})_3](BF_4)_3$ R = Ph complexes. The phenyl substituents on oxazoline moieties and tetrafluoroborate anions have been omitted for clarity.

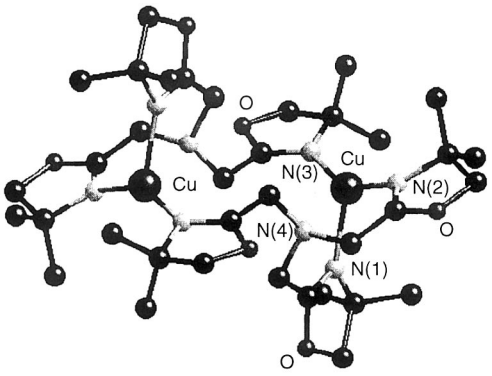

Fig. 58. Molecular structure of $[Cu(\mathbf{44})]_2(BF_4)_2$. The tetrafluoroborate anions have been omitted for clarity.

neutral macrocyclic ligands was obtained. This complex showed the Ag_4 core in a notably distorted trigonal-planar arrangement, in which both the carbonyl oxygen atoms and the dihydrooxazole nitrogens coordinated the silver atoms [144].

The naturally occurring cyclic peptide ascidiacyclamide contains two oxazoline and two thiooxazoline rings, which with copper(II) salts gave a binuclear complex $[Cu_2(ascidH_2)(1,2\text{-}\mu\text{-}CO_3)(H_2O)_2] \cdot 2H_2O$ [145] (Fig. 61). The magnetic moment is close to that expected for two isolated d^9 copper(II) ions at r.t. Variable-temperature susceptibility measurements showed the existence of a weak ferromagnetic coupling. The crystal stucture showed pentacoordinate copper ions in a distorted square-based pyramid with an assumed carbonate bridge. In the preparation of the complex, copper(II) nitrate was used while carbonate was not introduced into the reaction media. So, since the binuclear complex is neutral, equilibration of the charge meant that the CO_3^{2-} anion had to be present. The simulation of the X-band EPR spectra of frozen methanol solutions of the binuclear complex suggests significant differences from the X-ray crystal structure. Changes in the symmetry of the copper ion and a decrease in the intramolecular Cu–Cu distance (3.60 from 4.43 Å) indicates a reorganization of the binuclear complex in methanol solutions.

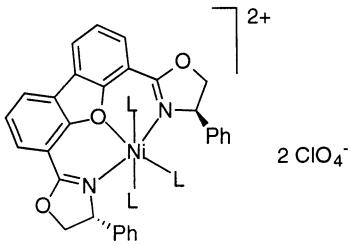

L = H_2O

Fig. 59. Hexacoordinated Ni(II) complex with terdentate **47** ligand.

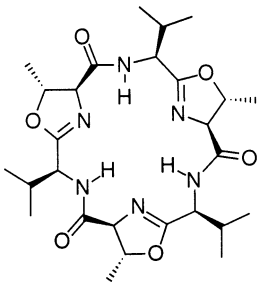

Fig. 60. Free cyclopeptide ligand.

Complexes of Rh(III) [$RhCl_2$(**NCN**)L] (L = H_2O, *t*-BuNC) [146] or Pd(II) [PdL(**NCN**)] (L = Cl, Br, I, H_2O) [93,147] containing a tridentate anionic **NCN** ligand were prepared by *ortho*-metalation when X = H [113,147], transmetalation reactions from ligands with X = Li [148] or $SnMe_3$ [146], and oxidative addition when X = Br or I [93] (Scheme 12).

The coordination can be deduced from the ^{1}H NMR spectrum from the absence of the signal corresponding to the proton located in *ortho* position to both oxazoline groups. An additional argument is the decrease, by about 35 cm^{-1}, from the free ligand of the ν(C=N) IR absorption, indicative of nitrogen coordination with the metal. The ligand has a C_2-symmetrical disposition that is maintained in solid state, as confirmed by X-ray molecular structure determination.

Palladium cationic complexes were obtained by treating the neutral complexes with silver salts in the presence of water. These complexes were tested in several catalytic reactions [147].

Some potentially tetradentate ligands (**N_4**) were reported (Chart 9) and complexes of Ru(II)-**48** [148,149], Pd(II)-**49**,**50** [150,151] and Ni(II)-**50** [151] are known.

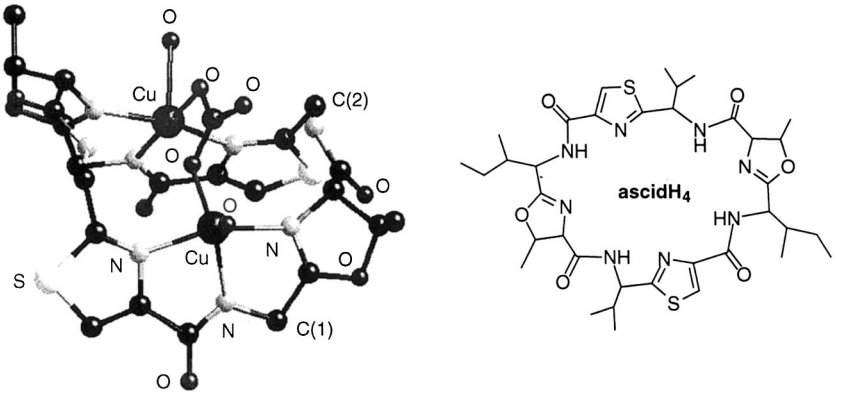

Fig. 61. Molecular structure of [Cu_2(ascidH_2)(1,2-μ-CO_3)(H_2O)$_2$] · 2H_2O. Substituents on C(1) and C(2) atoms have been omitted for clarity.

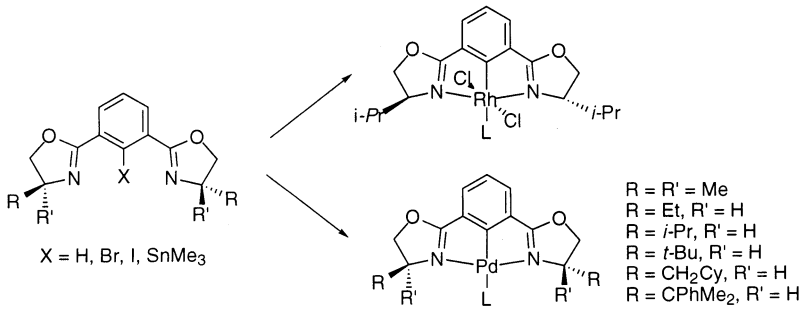

Scheme 12.

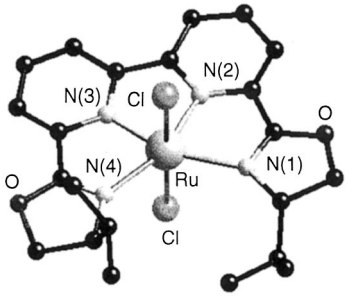

Fig. 62. Molecular structure of $[RuCl_2(\mathbf{48})]$ (R = *i*-Pr).

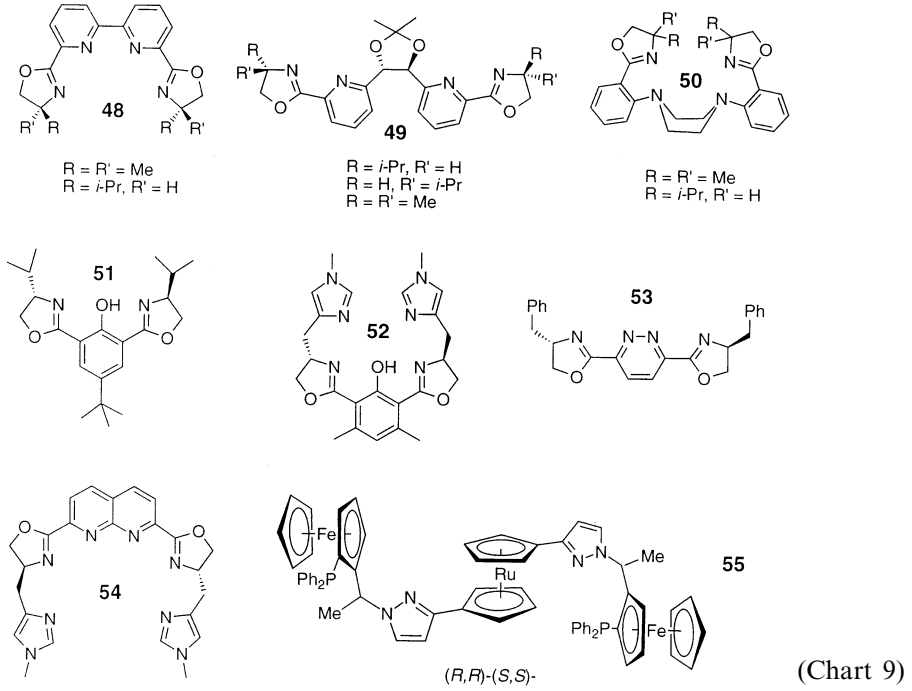

(Chart 9)

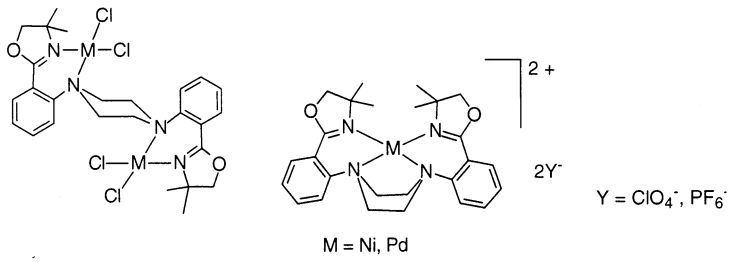

Fig. 63. Coordinating behavior of the bis(oxazoline)-bis(amine) ligands.

Neutral ruthenium complexes with tetradentate bis(oxazoline)-bipy ligands were obtained. The crystal structure of the dark red [$RuCl_2$(**48**)] complex (**48**, R = *i*-Pr) was determined [148]. The ligand showed C_2 symmetry in a distorted octahedral Ru environment; the N(1)–Ru–N(4), N(1)–Ru–N(2) and N(2)–Ru–N(3) bond angles are 124.1, 77.6 and 81.2°, respectively. The Ru–N(1) and Ru–N(4) bonds are longer (2.189 and 2.151 Å) than the Ru–N(2) and Ru–N(3) bonds (1.927 and 1.938 Å), suggesting a less stable oxazoline–Ru link in a highly strained environment (Fig. 62).

The ^{1}H NMR in solution also showed well-defined signals according to the C_2 symmetry. However, the strain of the oxazoline–Ru bond led to the formation of a new complex [$RuCl_2(CO)(\kappa^3$-**48**)], when complex [$RuCl_2$(**48**)] (**48**, R = *i*-Pr) was treated with carbon monoxide at 70°C. No further addition of carbon monoxide was observed and therefore a strong tridentate linkage of the **48** ligand was assumed. Electrochemical studies were also performed [149,150].

Chelucci tested $\mathbf{N_4}$ ligands (**49**) in the enantioselective palladium catalyzed allylic substitution reaction [150]. The results showed that the chirality of the dioxolane backbone is responsible for the stereoselectivity of the reaction. The substituents of the oxazoline ring were not however important. Chelucci tentatively suggested that the ligand coordinated with the palladium in a bis-bidentate fashion.

When a bis(oxazoline)-bis(amine) ligand (**50**) was used in the preparation of Ni(II) and Pd(II) complexes [151], the ligand gave binuclear neutral complexes and mononuclear cationic compounds with the ligand coordinating the metal ions in a bis-bidentate or tetradentate fashion respectively (Fig. 63). The neutral complexes are stable in solid state, but in solution decoordination takes place very rapidly. This process might be followed by ^{1}H NMR with the palladium compound. The neutral nickel complex is paramagnetic (2 e^-) without any interaction between the two metal centers, according to a tetrahedral environment of the nickel atom.

Recently the coordination behavior of chiral polydentate ligands (**51**–**54**) with Zn(II), Ni(II) and Cu(II) has been investigated [152]. The formation of a 1:1 complex between $ZnCl_2$ and ligand **51** was supported by NMR experiments (Fig. 64a). However, when the sodium salt of **51** was used instead, a binuclear complex [Zn_2(**51**)$_3$]Cl was obtained. The X-ray analysis of suitable crystals showed the structure of the complex in a C_3-symmetric arrangement with oxygen bridges. The analogous nickel

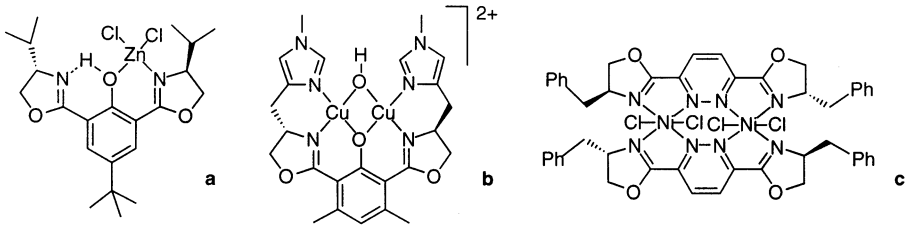

Fig. 64. Coordination behavior of **51**–**53** ligands.

compound was also obtained. Treatment of ligand **52** with $Cu(ClO_4)_2 \cdot 6H_2O$ in methanol gave the dinuclear complex (Fig. 64b), as confirmed by X-ray analysis.

The complexation of ligand **53** was studied with titration experiments, followed by NMR and UV spectroscopy of Zn(II) and Ni(II) salts. The results were consistent with a dimeric species (Fig. 64c) in equilibium with free ligand and metal dichloride. The crystal structure determination of the binuclear nickel compound confirmed the expected structure. With ligand **54**, crystalline Ni(II) and Cu(II) compounds were prepared. X-ray crystal analysis was carried out with the nickel compound, showing a binuclear molecular structure $[Ni_2(\mu\text{-}AcO)_2(H_2O)_2(\mathbf{54})](ClO_4)_2$. The preparation of the copper complex, under the same conditions, led to a different species. IR and mass spectra suggested a binuclear complex, with one or two perchlorate ions coordinated to the metal centers '$Cu_2(ClO_4)_4(H_2O)_4(\mathbf{54})$'.

Togni et al. described bimetallic palladium complexes with **PNNP** (**55**) ligands. These proved to be effective catalysts in allylic substitution reactions [153]. In these complexes, the ligand acts as a bridge between two palladium centers, and for each metallic atom a P–N chelate is formed. In our laboratory, we prepared chiral $\mathbf{N_2P_2}$ ligands, containing four stereocenters (two chiral carbon and two chiral phosphorus atoms), from dppe and dppp diphosphines, with *ortho*-oxazolinyl substituent on phenyl group (Eq. (19)). We synthesized and characterized ionic allylic palladium compounds, $[Pd_2(allyl)_2(\mu\text{-}\mathbf{N_2P_2})](PF_6)_2$, which gave very good asymmetric inductions in allylic alkylations [154]. The crystal structure of $[Pd_2(\eta^3\text{-}2\text{-}Me\text{–}C_3H_4)_2(\mu\text{-}\mathbf{N_2P_2})](PF_6)_2$ ($\mathbf{N_2P_2}$, R = Et) was resolved (Fig. 65). The geometry around the palladium atoms is distorted square-planar (the bite angles P(1)–Pd(1)–N(1) and P(2)–Pd(2)–N(2) are 88.3 and 89.4°, respectively) and the bond lengths Pd–N and Pd–P are in the range of published values for this type of distance (ca. Pd–N and Pd–P are 2.0 and 2.3 Å, respectively). As mentioned for other palladium–**NP** systems, the greater *trans* influence of phosphorus atoms than that shown by nitrogen atoms is found for the longer distances Pd–C(allylic terminus).

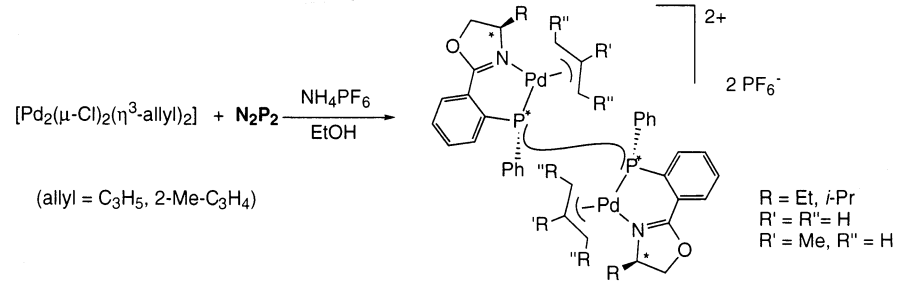

(19)

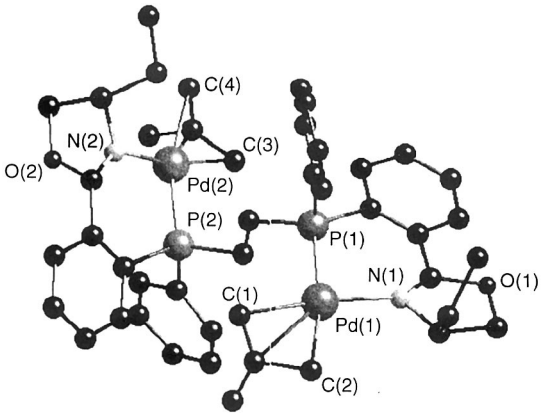

Fig. 65. Molecular structure of $[Pd_2(\eta^3\text{-}2\text{-}Me{-}C_3H_4)_2(\mu\text{-}\mathbf{N_2P_2})](PF_6)_2$. The hexafluorophosphate anions have been omitted for clarity.

Bimetallic palladium species have also been obtained by double metallation of the 1,4-bis[(4′*R*)-(4′-ethyl-3′,4′-dihydroxazol-2′-yl)]benzene, in spite of the two electron-withdrawing oxazoline substituents on the phenyl group (Eq. (20)) [113].

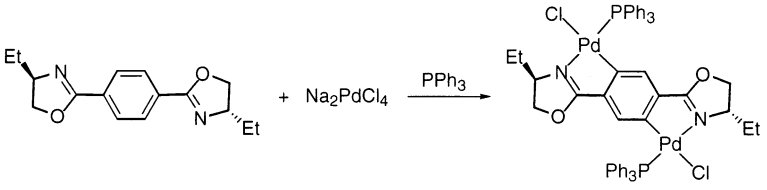

(20)

4. Other metal complexes

As mentioned in the Introduction, the aim of this review is to highlight the main structural aspects of transition metal complexes with ligands containing oxazoline groups. The literature shows that these compounds have been extensively studied in an attempt to discover their catalytic applications. However, in the last decade, s- and p-block metal complexes coordinated with oxazolines have also been reported because of their potential as active catalysts in processes catalyzed by Lewis acids, including Diels–Alder additions or aldol reactions. Structural data for lanthanides and actinides are not available, although for uranium(VI) and thorium(IV) ions some complexes with benzoxazoles have recently been described [155].

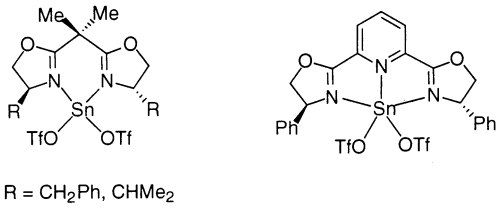

R = CH_2Ph, $CHMe_2$

Fig. 66. Tetra- and pentacoordinated tin complexes.

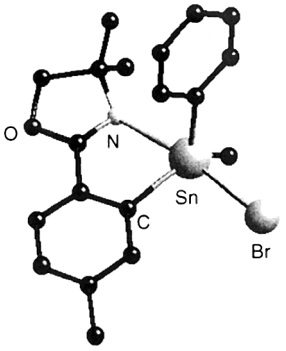

Fig. 67. Molecular structure of [Sn(**NC**)BrMePh].

For p-block metals, Evans and co-workers studied catalytic enantioselective aldol additions, where the catalytic precursors are neutral Sn(II) complexes with chiral bis(oxazoline) and pybox ligands, [$Sn(OTf)_2$(**37**)] (**37**, R = Bn, *i*-Pr) and [$Sn(OTf)_2$(**42**)] (**42**, R = Ph) (Fig. 66) [156].

For pybox complex, the X-ray structure was solved, showing Ψ-octahedral geometry for the tin atom with distortion of the triflate groups away from the active Sn(II) lone pair.

Organometallic tin(IV) compounds were also characterized, both in the solid state and in solution [157,158]. The first organotin complexes containing an oxazoline ligand were reported by van Koten and co-workers (Eq. (21)) [157]. The crystal structure of [Sn(**NC**)BrMePh] shows that the metal atom has trigonal bipyramidal coordination geometry, containing a *C,N*-cyclometalated ring (the bite angle N–Sn–C is 75.5°), where the carbon atoms are at the equatorial positions, and the more electronegative atoms (nitrogen and bromine) are at the axial sites (Fig. 67). Also, ^{119}Sn NMR studies showed that pentacoordination around the tin atom is retained in solution for series of stannylates thiophenes containing oxazoline and pyridine fragments [158].

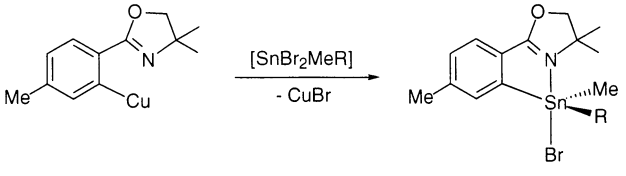

R = Me, Ph (21)

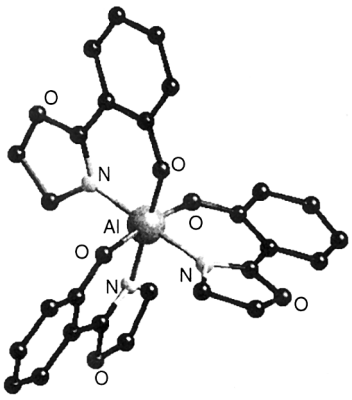

Fig. 68. Molecular structure of [Al(**NO**)$_3$].

Coordination chemistry of oxazoline ligands with Group 13 metal ions obtained neutral complexes which contain three anionic chelate rings, [M(**NO**)$_3$] (M = Ga, In, Tl; the **NO** ligands differ in the substituents on the oxazoline cycle) (Fig. 68) [12b,159]. The geometry around the metal ions is a slightly distorted octahedron (bite angles N–Al–O in the range 87.3–89.9°, similar to those reported for analogous [Mn(**NO**)$_3$] [50]), while the metal cycle is coplanar to the oxazoline and phenyl ring.

With ligand **36** (R = *i*-Pr, *t*-Bu, Ph), the structures of neutral magnesium(II) complexes were determined by means of IR and NMR spectroscopies. These data indicate that the C_2 symmetrical bis(oxazolines) are coordinated with the metal through both nitrogen atoms. The molecular weight measurements suggest dimeric and monomeric compounds, [MgX(**36**)]$_2$ (X = Cl, ethyl) and [Mg(**36**)$_2$] [160]. Also, some theoretical and solution chemistry studies with magnesium complexes were undertaken, in order to explain the diastero- and enantio-selectivity in several addition processes [161].

5. Conclusions

Given its metal coordination, the oxazoline fragment is potentially a versatile Lewis base. The oxazoline group moreover shows several coordinating modes: monodentate, bidentate, polydentate, bridge. In general it is coordinated to its metal center via the nitrogen donor atom, although a few examples have been described in which the oxazoline fragment is formed by deprotonation of an aminooxycarbene ligand and therefore, bonded by the iminic carbon atom [21–23]. Even in this latter case, the ease with which dimeric species form illustrates the coordinating ability of the iminic nitrogen. No complexes have been reported in which the oxygen of the oxazoline moiety acts as the donor atom. In the [Cu(**NO**)$_2$]

complex, where a pseudopentacoordinate copper atom is present in the crystal structure (Fig. 16), the coordination sphere is formed from the two bidentate ligands and completed by a long-distance interaction between the copper and the oxygen atom of the phenolato fragment of an adjacent molecule [44].

The coordination of the oxazoline ligand may be monitored by IR spectroscopy in the 1600 cm^{-1} zone. Upon coordination the ν(C=N) generally shifts towards lower frequencies (ca. 30 cm^{-1}).

In the metallic complexes, the mean bond angles of the oxazoline ring (**1–2–3**, **2–1–5**, **1–5–4**, **3–4–5**, **2–3–4**, Fig. 1) do not differ significantly (117.15, 106.13, 104.52, 102.29 and 107.75°, respectively, for statistical analysis of 63 structures) from that of the free ligands, ca. 1° (Table 1). However, the bond distances **2–3** and **3–4** (1.28 and 1.49 Å, respectively) are slightly longer than their counterparts, while **1–5** and **1–2** (1.52 and 1.34 Å, respectively) are shorter, though the bond length between the two sp^3 carbon atoms is invariable. These data point to a weak π-acceptor behavior of this kind of ligand when bonded to metallic centers. This trend has also been observed in solution by NMR spectroscopy [92].

The planarity of the heterocycle should also be noted, although the mean torsion angles are slightly higher than those recorded for the free oxazolines: **5–1–2–3** and **4–3–2–1** are 5.40 and 3.67°, respectively.

In spite of the hybridization of the oxazolynic nitrogen atom and the strain suffered by the heterocyclic five-membered ring, the 2-oxazoline ligands can stabilize a number of metallic ring sizes in polydentate ligands, demonstrating the electronic 'flexibility' of the nitrogen atom, which contributes to the stability of the complexes. The angle M–N(2)–C(2) (Fig. 69) is sensitive to the chelate ring size, showing a relatively wide range of mean values: from 112.88 to 125.79° for five- and six-membered rings, respectively. Furthermore, there are no differences between M–N(1)–C(1) and M–N(2)–C(2) angles in **NN′** ligands (114.09 and 114.68° respectively, mean values of five complexes). These values are analogous to those observed in the Pd–N–C(1) angles in bipyrine palladium complexes (114.7°, mean value of 78 structures in mononuclear complexes). Thus, no constant effect is observed on the coordination of the nitrogen atoms as the ring size of the ligand varies.

A large number of oxazolines ligands are 2-aryl substituted. The trend to coplanarity between the oxazoline moiety and the aromatic group observed for the free ligands (see Section 2) can also be seen in the chelate cycles, suggesting a certain degree of electron delocalization. For the six-membered rings with anionic **NO** ligands, both groups are coplanar (2–5°), but for six-membered chelate rings with neutral **NP** ligands, the deviation of the coplanarity is large. The twist in the

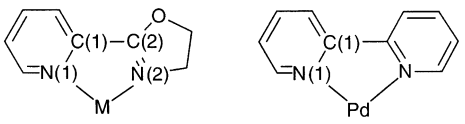

Fig. 69. Atom labeling of the five-membered chelate rings.

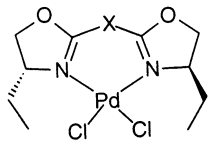

Fig. 70. Model of the palladium structure used for geometrical calculations.

phenyl bridge in relation to the oxazoline double bond can reach 38.7°, probably due to the steric hindrance of the substituents on the phosphorus atom. Nevertheless, the average bond distance **2–6** (Fig. 1), 1.46 Å (from 27 structures), is only slightly shorter than the C_{sp^2}–C_{sp^2} single bond (1.48 Å, [13]). However, in monodentate aryloxazolines substituted on the sp^2 carbon, the aryl moiety is twisted between 25 and 56.5° in relation to the iminic double bond. Thus, it would seem that steric requirements are determinant.

Generally, the bite angles (N–M–Y), fall within the range 80–90° for five-, six- and seven-membered cycles, where Y is a non-metal atom (C, N, O, S, P). These values are higher for nine-membered rings with strained backbones, such as binaphthyl (100.3° [117]) and diphenyl groups (134° [111]). Geometrical optimization of the chelate ring size in the palladium complex (Fig. 70) by simple PM3 calculation [162] shows the tendency of the system to relax as the size of the chelate ring increases (Table 3). The experimental mean values follow the same trend: 79.11° (15 structures), 85.24° (33 structures) and 91.00° (one structure) for metal transition complexes with five-, six- and seven-membered metallic rings, respectively. This calculation also reveals an increase in the stability of these complexes as the number of CH_2 groups between the two oxazoline moieties and the flexibililty of the bridge X group increase.

In catalytic processes, the proximity of the substituent on position **4** (Fig. 1) to the coordination sphere is also a significant factor. This effect can be observed tentatively by analyzing the distances between the metal and the carbon C* (Fig. 71).

The results for five-, six-, seven- and nine-membered rings [11] demonstrate the approximation of the substituent on the chiral carbon bonded directly to the oxazoline nitrogen atom to the metal when the chelate ring size increases (cluster complexes have been excluded from this evaluation). This is one of the arguments used to explain the increase of the selectivity of the catalytic reactions that follow this trend.

Table 3
ΔH_f (kcal/mol) and bite angle (°) values for palladium symmetric bis(oxazoline) complexes (Fig. 70)

X	Ring size	ΔH_f	N–Pd–N
–	5	−165.47	87.12
CH_2	6	−178.89	93.47
CH_2–CH_2	7	−195.23	92.07
CH=CH	7	−159.52	92.28

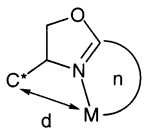

n = 5, d = 3.855 Å (10)
n = 6, d = 3.764 Å (30)
n = 7, d = 3.680 Å (1)
n = 9, d = 3.777 Å (1)

Fig. 71. Mean distance values between M–C* for chelate complexes (the number of structures from CSD data [11] is shown in parentheses).

Few systematic studies on ligand substitution reactions in oxazoline complexes have been conducted, though it has been demonstrated that oxazoline ligands are substituted by either monodentate or bidentate phosphines. Nevertheless, examples have been reported in which the oxazoline ligand is substituted by other Lewis bases such as carbon monoxide, dithiocarbamate, isonitrile and pyridine.

Oxazoline complexes are usually stable in coordinating and non coordinating solvents but in some cases fluxional phenomena have been detected by ^{1}H NMR spectroscopy. This dynamic behavior is particularly common in palladium(II) chemistry with allylic organic groups, and believed by some authors to be a result of Pd–N bond breaking in complexes with bidentate ligands **NN** (symmetric bipyridine derivative ligands) [163] or **NN′** (pyrazol–azine ligands) [164]. However, to date, comparable studies for complexes with bidentate oxazolines ligands have not been reported. We have obseved by NOE experiments that the dynamic behavior of [Pd(η^3-allyl)(**NN′**)]BF_4 (**NN′** = **5**, **11**) is not related to the decoordination of the nitrogen atoms [40] but is rather associated with allylic rotation and/or $\pi-\sigma$ exchange. Bis(oxazoline) (**36**, **37**) ligands that form six-membered heterocyclic rings on coordination can be considered non-rigid. The NMR spectra of these Pd(II) complexes suggest two rapidly interconverting conformations of the chelate ring [100]. Complexes in which the bonding of a tridentate ligand (**42**) is restricted to a bidentate mode of coordination are potentially fluxional. Two possible mechanisms can be used to describe this interchange: either, the ligand might adopt a pseudo-terdentate bonding mode in the transition state, or, a cleavage of the outer *N*-bond might lead to the formation of an intermediate where the ligand is bonded to the metal only by the central *N*-donor atom [129].

References

[1] A. Togni, L.M. Venanzi, Angew. Chem. Int. Ed. Engl. 33 (1994) 497.
[2] A. Pfaltz, Acc. Chem. Res. 26 (1993) 339.
[3] A.K. Ghosh, P. Mathiavanan, J. Cappiello, Tetrahedron: Asymmetry 9 (1998) 1.
[4] (a) A. Pfaltz, Acta Chem. Scand. 50 (1996) 189. (b) C.J. Richards, A.J. Locke, Tetrahedron: Asymmetry 9 (1998) 2377.
[5] R. Andreasch, Monatsh. Chem. 5 (1884) 33.
[6] (a) R.H. Wiley, L.L. Bennett, Chem. Rev. 44 (1949) 447. (b) J.A. Frump, Chem. Rev. 71 (1971) 483.
[7] R.J. Bergeron, Chem. Rev. 84 (1984) 587.
[8] T.W. Greene, P.G.M. Wuts, Protective Groups in Organic Synthesis, 2nd ed., Wiley, New York, 1991, pp. 265–266 and 433–436.

[9] M. Reuman, A.I. Meyers, Tetrahedron 41 (1985) 837.
[10] (a) T.G. Gant, A.I. Meyers, Tetrahedron 50 (1994) 2297. (b) D.J. Ager, I. Prakash, D.R. Schaad, Chem. Rev. 96 (1996) 835. (c) M. Peer, J.C. de Jong, M. Keifer, T. Langer, H. Rieck, H. Schell, P. Sennhenn, J. Sprinz, H. Steinhagen, B. Wiese, G. Helmchen, Tetrahedron 52 (1996) 7547 and references therein.
[11] F.H. Allen, O. Kennard, Chem. Des. Autom. News 8 (1993) 31. Cambridge Structural Data, Version 5.15.
[12] (a) D.L. Eng-Wilmot, D. van der Helm, J. Am. Chem. Soc. 102 (1980) 7719. (b) H.R. Hoveyda, V. Karunaratne, S.J. Rettig, C. Orvig, Inorg. Chem. 31 (1992) 5408. (c) J.L. Serrano, T. Sierra, Y. González, C. Bolm, K. Weickhardt, A. Magnus, G. Moll, J. Am. Chem. Soc. 117 (1995) 8312.
[13] J. March, Advanced Organic Chemistry. Reactions, Mechanisms, and Structure, 3rd ed., Wiley, New York, 1985, pp. 18–19 and references therein.
[14] P. Alvarez Boo, E. Freijanes, E. Garcia Martinez, J.S. Casas, J. Sordo, Synth. React. Inorg. Met. Org. Chem. 25 (1995) 115.
[15] J.M. Valk, F. Maassarani, P. van der Sluis, A.L. Spek, J. Boersma, G. van Koten, Organometallics 13 (1994) 2320.
[16] T. Izumi, H. Watabe, A. Kasahara, Bull. Chem. Soc. Jpn. 54 (1981) 1711.
[17] R.A. Michelin, R. Bertani, M. Mozzon, G. Bombieri, F. Benetollo, R.J. Angelici, Organometallics 10 (1991) 1751.
[18] R.A. Michelin, R. Bertani, M. Mozzon, G. Bombieri, F. Benetollo, R.J. Angelici, J. Chem. Soc. Dalton Trans. (1993) 959.
[19] R.A. Michelin, M. Mozzon, P. Berin, R. Bertani, F. Benetollo, G. Bombieri, R.J. Angelici, Organometallics 13 (1994) 1341.
[20] L. Campardo, M. Gobbo, R. Rocchi, R. Bertani, M. Mozzon, R.A. Michelin, Inorg. Chim. Acta 245 (1996) 269.
[21] H. Motschi, R.J. Angelici, Organometallics 1 (1982) 343.
[22] S. Wang, R.J. Angelici, J. Organomet. Chem. 352 (1988) 157.
[23] (a) L. Zanotto, R. Bertani, R.A. Michelin, Inorg. Chem. 29 (1990) 3265. (b) R. Bertani, M. Mozzon, R.A. Michelin, F. Benetollo, G. Bombieri, T.J. Castilho, A.J.L. Pombeiro, Inorg. Chim. Acta 189 (1991) 175.
[24] G. Balavoine, J.C. Clinet, P. Zerbib, K. Boubeker, J. Organomet. Chem. 389 (1990) 259.
[25] G. Balavoine, J.C. Clinet, J. Organomet. Chem. 390 (1990) C84.
[26] G. Balavoine, J.C. Clinet, J. Organomet. Chem. 405 (1991) C29.
[27] P.A. Bonnardel, R.V. Parish, R.G. Pritchard, J. Chem. Soc. Dalton Trans. (1996) 3185.
[28] M. Desmet, H.G. Raubenheimer, G.J. Kruger, Organometallics 16 (1997) 3324.
[29] (a) G.W. Gschwend, A. Hamdan, J. Org. Chem. 40 (1975) 2008. (b) A.I. Meyers, E.D. Michelin, J. Org. Chem. 40 (1975) 3158.
[30] E. Wehman, G. van Koten, J.T.B.H. Jastrzebski, J. Organomet. Chem. 302 (1986) C35.
[31] E. Wehman, G. van Koten, J.T.B.H. Jastrzebski, M.A. Rotteveel, C.H. Stam, Organometallics 7 (1988) 1477.
[32] U. Koelle, K. Bücken, U. Englert, Organometallics 17 (1998) 1376.
[33] A.J. Davenport, D.L. Davies, J. Fawcett, S.A. Garrat, L. Lad, D.R. Russell, Chem. Commun. (1997) 2347.
[34] W.A. Herrmann, L.J. Goossen, M. Spiegler, Organometallics 17 (1998) 2162.
[35] H. Brunner, R. Störiko, F. Rominger, Eur. J. Inorg. Chem. (1998) 771.
[36] H. Brunner, U. Obermann, Chem. Ber. 122 (1989) 499.
[37] P. Segl'a, M. Jamnicky, Inorg. Chim. Acta 205 (1993) 221.
[38] G. Chelucci, S. Medici, A. Saba, Tetrahedron: Asymmetry 8 (1997) 3183.
[39] (a) K. Nordström, E. Macedo, C. Moberg, J. Org. Chem. 62 (1997) 1604. (b) K. Wärnmark, R. Sttrannl, M. Cernerud, I. Terrien, F. Rahm, K. Nordström, C. Moberg, Acta Chem. Scan. 52 (1998) 961.
[40] J.M. Canal, M. Gómez, M. Rocamora, G. Muller, J.C. Clinet, E. Duñach, D. Franco, A. Jiménez, F.H. Cano, to be submitted for publication.
[41] P.S. Pregosin, R. Salzmann, Coord. Chem. Rev. 155 (1996) 35 and references therein.

[42] N. Paschke, A. Röndigs, H. Poppenborg, J.E.A. Wolf, B. Krebs, Inorg. Chim. Acta 264 (1997) 239.
[43] T. Ichiyanagi, M. Shimizu, T. Fujisawa, Tetrahedron 53 (1997) 9599.
[44] C. Bolm, K. Weickhardt, M. Zehnder, D. Glassmaker, Helv. Chim. Acta 74 (1991) 717.
[45] M. Gómez-Simón, S. Jansat, G. Muller, D. Panyella, M. Font-Bardía, X. Solans, J. Chem. Soc. Dalton Trans. (1997) 375.
[46] H. Yang, M.A. Khan, K. Nicholas, J. Mol. Catal. 91 (1994) 319.
[47] H. Yang, M.A. Khan, K. Nicholas, Organometallics 12 (1993) 3485.
[48] C. Bolm, T.K.K. Luong, K. Harms, Chem. Ber. 130 (1997) 887.
[49] C. Bolm, T.K.K. Luong, G. Schlingloff, Synlett (1997) 1151.
[50] M. Hoogenraad, K. Ramkisoensing, H. Kooijman, A.L. Spek, E. Bouwman, J.G. Haasnot, J. Reedijk, Inorg. Chim. Acta 279 (1998) 217.
[51] K. Inamoto, M. Koikawa, M. Nakashima, T. Tokii, Inorg. Chim. Acta 249 (1996) 251.
[52] P.G. Cozzi, C. Floriani, A. Chiesi-Villa, C. Rizzoli, Inorg. Chem. 34 (1995) 2921.
[53] P.G. Cozzi, E. Gallo, C. Floriani, A. Chiesi-Villa, C. Rizzoli, Organometallics 14 (1995) 4994.
[54] E. Shuter, H.R. Hoveyda, V. Karanuratne, S.J. Rettig, C. Orvig, Inorg. Chem. 35 (1996) 368.
[55] R.W. Saalfrank, M. Decker, F. Hampel, K. Peters, H.G. von Schnering, Chem. Ber. 130 (1997) 1309.
[56] S. Bhaduri, N. Sapre, P.G. Jones, J. Organomet. Chem. 509 (1996) 105.
[57] G.J. Dawson, C.G. Frost, C.J. Martin, J.M.J. Williams, S.J. Coote, Tetrahedron Lett. 34 (1993) 7793.
[58] J.V. Allen, J.F. Bower, J.M.J. Williams, Tetrahedron: Asymmetry 5 (1994) 1895.
[59] A. Cheney, M.R. Bryce, Tetrahedron: Asymmetry 7 (1996) 3247.
[60] A. Cheney, M.R. Bryce, R.W.J. Chubb, A.S. Batsanov, J.A.K. Howard, Tetrahedron: Asymmetry 8 (1997) 2337.
[61] K. Boog-Wick, P.S. Pregosin, G. Trabesinger, Organometallics 17 (1998) 3254.
[62] P.J. Heard, D.A. Tocher, J. Organomet. Chem. 549 (1997) 295.
[63] G. Doisneau, G. Balavoine, T. Fillebeen-Khan, J.C. Clinet, J. Delaire, I. Ledoux, R. Loucif, G. Puccetti, J. Organomet. Chem. 421 (1991) 299.
[64] J.M.J. Williams, Synlett (1996) 705.
[65] G. Helmchen, S. Kudis, P. Sennhenn, H. Steinhagen, Pure Appl. Chem. 69 (1997) 513.
[66] G.C. Lloyd-Jones, A. Pfaltz, Z. Naturforsch. 50b (1995) 361.
[67] D. Carmona, C. Cativiela, S. Elipe, F.J. Lahoz, M.P. Lamata, M.P. López-Ram de Viu, L.A. Oro, C. Vega, F. Viguri, Chem. Commun. (1997) 2351.
[68] K.L. Bray, C.P. Butts, G.C. Lloyd-Jones, M. Murray, J. Chem. Soc. Dalton Trans. (1998) 1421.
[69] G.C. Lloyd-Jones, C.P. Butts, Tetrahedron 54 (1998) 901 and references therein.
[70] J. Sprinz, G. Helmchen, Tetrahedron Lett. 34 (1993) 1769.
[71] J. Sprinz, M. Kiefer, G. Helmchen, M. Reggelin, G. Hutter, O. Walter, L. Zsolnai, Tetrahedron Lett. 35 (1994) 1523.
[72] N. Baltzer, L. Macko, S. Schaffner, M. Zehnder, Helv. Chim. Acta 79 (1996) 803.
[73] S. Liu, J.F.K. Müller, M. Neuburger, S. Schaffner, M. Zehnder, J. Organomet. Chem. 549 (1997) 283.
[74] S. Schaffner, L. Macko, M. Neuburger, M. Zehnder, Helv. Chim. Acta 80 (1997) 463.
[75] S. Schaffner, J.F.K. Müller, M. Neuburger, M. Zehnder, Helv. Chim. Acta 81 (1998) 1223 and references therein.
[76] B. Reif, H. Steinhagen, B. Junker, M. Reggelin, C. Griesinger, Angew. Chem. Int. Ed. Engl. 37 (1998) 1903.
[77] H. Steinhagen, M. Reggelin, G. Helmchen, Angew. Chem. Int. Ed. Engl. 36 (1997) 2108.
[78] B. Wiese, G. Helmchen, Tetrahedron Lett. 39 (1998) 5727.
[79] M. Ogasawara, K. Yoshida, H. Kamei, K. Kato, Y. Uozomi, T. Hayashi, Tetrahedron: Asymmetry 9 (1998) 1779.
[80] Y. Imai, W. Zhang, T. Kida, Y. Nakatsuji, I. Ikeda, Tetrahedron Lett. 39 (1998) 4343.
[81] C.P. Richards, D.E. Hibbs, M.B. Hursthouse, Tetrahedron Lett. 36 (1995) 3745.
[82] K.H. Ahn, C.W. Cho, J. Park, S. Lee, Tetrahedron: Asymmetry 8 (1997) 1179.

[83] Y. Nishibayashi, I. Takei, S. Uemura, M. Hidai, Organometallics 17 (1998) 3420.
[84] K.H. Ahn, C.W. Cho, H.H. Baek, J. Park, S. Lee, J. Org. Chem. 61 (1996) 4937 and references therein.
[85] J. Park, S. Lee, K.H. Ahn, C.W. Cho, Tetrahedron Lett. 40 (1995) 7263.
[86] M. Sperrle, A. Aeby, G. Consiglio, A. Pfaltz, Helv. Chim. Acta 79 (1996) 1387.
[87] A. Aeby, F. Bangerter, G. Consiglio, Helv. Chim. Acta 81 (1998) 764.
[88] R. Prétot, A. Pfaltz, Angew. Chem. Int. Ed. Engl. 37 (1998) 323.
[89] P. Schnider, G. Koch, R. Prétot, G. Wang, F.M. Bohnen, C. Krüger, A. Pfaltz, Chem. Eur. J. 3 (1997) 887.
[90] (a) D.A. Evans, K.A. Woerpel, M.J. Scott, Angew. Chem. Int. Ed. Engl. 31 (1992) 430. (b) D.M. Haddleton, D.J. Duncal, A.J. Clark, M.C. Crossman, D. Kukulj, New J. Chem. (1998) 315.
[91] M.G. Burnett, V. Mckee, S.M. Nelson, J. Chem. Soc. Dalton Trans. (1981) 1492.
[92] C.A. Merlic, B. Adams, J. Organomet. Chem. 431 (1992) 313.
[93] S.E. Denmark, R.A. Stavenger, A.-M. Faucher, J.P. Edwards, J. Org. Chem. 62 (1997) 3375.
[94] M. Onishi, K. Isagawa, Inorg. Chim. Acta 179 (1991) 155.
[95] G. van Koten, K. Vrieze, Adv. Organomet. Chem. 21 (1982) 151 and references therein.
[96] (a) J.M. Brown, P.J. Guiry, D.M. Price, M.B. Hursthouse, S. Karalulov, Tetrahedron: Asymmetry 5 (1994) 561. (b) J. Hall, J.-M. Lehn, A. DeCian, J. Fischer, Helv. Chim. Acta 74 (1991) 1.
[97] R.P. Singh, Synth. React. Inorg. Met. Org. Chem. 27 (1997) 155.
[98] S. Bennett, S.M. Brown, G. Conole, M. Kessler, S. Rowling, E. Sinn, S. Woodward, J. Chem. Soc. Dalton Trans. (1995) 367.
[99] U. Leutenegger, G. Umbricht, C. Fahrni, P. von Matt, A. Pfaltz, Tetrahedron 48 (1992) 2143.
[100] P. von Matt, G.C. Lloyd-Jones, A.B.E. Minidis, A. Pfaltz, L. Macko, M. Neuburger, M. Zehnder, H. Rüegger, P.S. Pregosin, Helv. Chim. Acta 78 (1995) 265.
[101] (a) P.S. Pregosin, C. Ammann, Pure Appl. Chem. 61 (1989) 1771. (b) A. Albinati, R.W. Kunz, C. Ammann, P.S. Pregosin, Organometallics 9 (1990) 1826.
[102] M. Zehnder, M. Neuburger, Acta Crystallogr. Sect. C 51 (1995) 1109.
[103] K. Ohkita, H. Kurosawa, T. Hasegawa, T. Hirao, I. Ikeda, Organometallics 12 (1993) 3211.
[104] M. Brookhart, M.I. Wagner, J. Am. Chem. Soc. 118 (1996) 7219.
[105] (a) D.A. Evans, M.C. Kozlowski, J.S. Tedrow, Tetrahedron Lett. 37 (1996) 7481. (b) D.A. Evans, G.S. Peterson, J.S. Johnson, D.M. Barnes, K.R. Campos, K.A. Woerpel, J. Org. Chem. 63 (1998) 4541.
[106] J.M. Takacs, E.C. Lawson, M.J. Reno, M.A. Youngman, D.A. Quincy, Tetrahedron: Asymmetry 8 (1997) 3073.
[107] L.F. Szczepura, S.M. Maricich, R.F. See, M.R. Churchill, K.J. Takeuchi, Inorg. Chem. 34 (1995) 4198.
[108] H. Asano, K. Katayama, H. Kurosawa, Inorg. Chem. 35 (1996) 5760.
[109] D.P. Goldberg, J. Telser, C.M. Bastos, S.J. Lippard, Inorg. Chem. 34 (1995) 3011.
[110] (a) R.E. Lowenthal, A. Abiko, S. Masamune, Tetrahedron Lett. 31 (1990) 6005. (b) D.A. Evans, K.A. Woerpel, M.M. Hinman, M.M. Faul, J. Am. Chem. Soc. 113 (1991) 726. (c) D. Müller, G. Umbricht, B. Weber, A. Pfaltz, Helv. Chim. Acta 74 (1991) 232.
[111] T.G. Gant, M.C. Noe, E.J. Corey, Tetrahedron Lett. 36 (1995) 8745.
[112] C. Bolm, K. Weickhardt, M. Zehnder, T. Ranff, Chem. Ber. 124 (1991) 1173.
[113] A. El Hatimi, M. Gómez, S. Jansat, G. Muller, M. Font-Bardía, X. Solans, J Chem. Soc., Dalton Trans. (1998) 4229.
[114] *aR* and *aS* means the configuration of the chiral axis, following the Cahn–Ingold–Prelog rules: R.S. Cahn, C. Ingold, V. Prelog, Angew. Chem. Int. Ed. Engl. 5 (1966) 385.
[115] A. Llobet, E. Plantalech, M. Gómez, G. Muller, H. Stoeckli-Evans, to be submitted for publication.
[116] Y. Imai, W. Zhang, T. Kida, Y. Nakatsuji, I. Ikeda, Tetrahedron Lett. 38 (1997) 2681.
[117] Y. Uozumi, K. Kato, T. Hayashi, J. Org. Chem. 63 (1998) 5071.
[118] (a) A.M. Harm, J.G. Knight, G. Stemp, Synlett (1996) 677. (b) I.W. Davies, L. Gerena, L. Castonguay, C.H. Senanayake, R.D. Larsen, T.R. Verhoeven, P.J. Reider, Chem. Commun. (1996) 1753. (c) I.W. Davies, L. Gerena, D. Cai, R.D. Larsen, T.R. Verhoeven, P.J. Reider,

Tetrahedron Lett. 38 (1997) 1145. (d) S.-G. Kim, C.-W. Cho, K.H. Ahn, Tetrahedron: Asymmetry 8 (1997) 1023. (e) J.M. Takacs, D.A. Quincy, W. Shay, B.E. Jones, C.R. Ross, Tetrahedron: Asymmetry 8 (1997) 3079. (f) C. Ching Mak, H.-F. Chow, Macromolecules 30 (1997) 1228. (g) H.-F. Chow, C. Ching Mak, J. Org. Chem. 62 (1997) 5116.
[119] X. Hua, M. Shang, A.G. Lappin, Inorg. Chem. 36 (1997) 3735.
[120] S.B. Park, H. Nishiyama, Y. Itoh, K. Itoh, Chem. Commun. (1994) 1315.
[121] H. Nishiyama, S.B. Park, K. Itoh, Chem. Lett. (1995) 599.
[122] S.B. Park, N. Sakata, H. Nishiyama, Chem. Eur. J. 2 (1996) 303.
[123] H. Nishiyama, K. Aoki, H. Itoh, T. Iwamura, N. Sakata, O. Kurihara, Y. Motoyama, Chem. Lett. (1996) 1071.
[124] (a) H. Nishiyama, Y. Itoh, H. Matsumoto, S.B. Park, K. Itoh, J. Am. Chem. Soc. 116 (1994) 2223. (b) H. Nishiyama, Y. Itoh, Y. Sugawara, H. Matsumoto, K. Aoki, K. Itoh, Bull. Chem. Soc. Jpn. 68 (1995) 1247.
[125] Y. Motoyama, K. Murata, O. Kurihara, T. Naitoh, K. Aoki, H. Nishiyama, Organometallics 17 (1998) 1251.
[126] H. Nishiyama, H. Sakaguchi, T. Nakamura, M. Horlhata, M. Kondo, K. Itoh, Organometallics 8 (1989) 846.
[127] H. Nishiyama, M. Kondo, T. Nakamura, S.B. Park, K. Itoh, Organometallics 10 (1991) 500.
[128] P.J. Heard, D.A. Tocher, J. Chem. Soc. Dalton Trans. (1998) 2169.
[129] P.J. Heard, C. Jones, J. Chem. Soc. Dalton Trans. (1997) 1083.
[130] D.A. Evans, J.A. Murry, P. von Matt, R.D. Norcross, S.J. Miller, Angew. Chem. Int. Ed. Engl. 34 (1995) 798.
[131] D.A. Evans, M.C. Kozlowski, J.S. Tedrow, Tetrahedron Lett. 37 (1996) 7481 and references therein.
[132] D.A. Evans, J.A. Murry, M.C. Kozlowski, J. Am. Chem. Soc. 118 (1996) 5814.
[133] D.A. Evans, M.C. Kozlowski, C.S. Burgey, D.W.C. MacMillan, J. Am. Chem. Soc. 119 (1997) 7893.
[134] A. Dattagupta, D. Bhuniya, V.K. Singh, Tetrahedron 50 (1994) 13725.
[135] A. Dattagupta, V.K. Singh, Tetrahedron Lett. 37 (1996) 2633.
[136] R. Nesper, P.S. Pregosin, K. Püntener, M. Wörle, Helv. Chim. Acta 76 (1993) 2239.
[137] R. Nesper, P.S. Pregosin, K. Pünterer, M. Wörle, A. Albinati, J. Organomet. Chem. 507 (1996) 85.
[138] C. Provent, S. Hewage, G. Brand, G. Bernardinelli, L.J. Charbonnière, A.F. Williams, Angew. Chem. Int. Ed. Engl. 36 (1997) 1287.
[139] Y. Jiang, Q. Jiang, X. Zhang, J. Am. Chem. Soc. 120 (1998) 3817.
[140] T.N. Sorrell, F.C. Pigge, P.S. White, Inorg. Chim. Acta 210 (1993) 87.
[141] Y. Jiang, Q. Jiang, G. Zhu, X. Zhang, Tetrahedron Lett. 38 (1997) 215.
[142] S. Kanemasa, Y. Oderaotoshi, H. Yamamoto, J. Tanaka, E. Wada, D.P. Curran, J. Org. Chem. 62 (1997) 6454.
[143] S. Kanemasa, Y. Oderaotoshi, S. Sakaguchi, H. Yamamoto, J. Tanaka, E. Wada, D.P. Curran, J. Am. Chem. Soc. 120 (1998) 3074.
[144] P. Wipf, S. Venkatraman, C.P. Miller, S.J. Geib, Angew. Chem. Int. Ed. Engl. 33 (1994) 1516.
[145] A.L. van den Brenk, K.A. Byriel, D.P. Fairlie, L.R. Gahan, G.R. Hanson, C.J. Hawkins, A. Jones, C.H.L. Kennard, B. Moubaraki, K.S. Murray, Inorg. Chem. 33 (1994) 3549.
[146] Y. Motoyama, N. Makihara, Y. Mikami, K. Aoki, H. Nishiyama, Chem. Lett. (1997) 951.
[147] M.A. Stark, C.J. Richards, Tetrahedron Lett. 38 (1997) 5881.
[148] H. Nishiyama, S.B. Park, M. Haga, K. Aoki, K. Itoh, Chem. Lett. (1994) 1111.
[149] K. Mizushima, M. Nakaura, S.B. Park, H. Nishiyama, H. Monjushiro, K. Harada, M. Haga, Inorg. Chim. Acta 261 (1997) 175.
[150] G. Chelucci, Tetrahedron: Asymmetry 8 (1997) 2667.
[151] M. Gómez, G. Muller, D. Panyella, M. Rocamora, E. Duñach, S. Olivero, J.C. Clinet, Organometallics 16 (1997) 3900.
[152] C.J. Fahrni, A. Pfaltz, M. Neuburger, M. Zehnder, Helv. Chim. Acta 81 (1998) 507.
[153] U. Burckhardt, M. Baumann, G. Trabesinger, V. Gramlich, A. Togni, Organometallics 16 (1997) 5252.

[154] M. Gómez, G. Muller, D. Panyella, P.W.N.M. van Leeuwen, P. Kamer, K. Goubitz, J. Fraanje, to be submitted for publication.
[155] (a) Chem. Abstr. 125 (1996) 47538w. (b) P.S. Mansingh, R.R. Mohanty, S. Jena, K.C. Dash, Indian J. Chem. Sect. A: Inorg. Bio-Inorg. Phys. Theor. Anal. Chem. 35A (1996) 479.
[156] D.A. Evans, D.W.C. MacMillan, K.R. Campos, J. Am. Chem. Soc. 119 (1997) 10859.
[157] J.T.B.H. Jastrzebski, E. Wehman, J. Boersma, G. van Koten, K. Goubitz, D. Heijdenrijk, J. Organomet. Chem. 409 (1991) 157.
[158] K. Mun Lo, S. Selvaratnam, S. Weng Ng, C. Wei, V.G. Kumar Das, J. Organomet. Chem. 430 (1992) 149.
[159] H.R. Hoveyda, C. Orvig, S.J. Rettig, Acta Crystallogr. Sect. C 50 (1994) 1906.
[160] R.P. Singh, Spectrochim. Acta Part A 53 (1997) 1713.
[161] (a) K.V. Gothelf, R.G. Hazell, K.A. Jørgensen, J. Org. Chem. 61 (1996) 346. (b) R.E. Gawley, P. Zhang, J. Org. Chem. 61 (1996) 8103.
[162] MacSpartan Plus version 1.1.7 from Wavefunction, Inc.
[163] A. Gogoll, J. Ornebro, H. Grennberg, J.E. Backvall, J. Am. Chem. Soc. 116 (1994) 3631.
[164] J. Elguero, A. Fruchier, A. de la Hoz, F.A. Jalón, B.R. Manzano, A. Otero, F. Gómez de la Torre, Chem. Ber. 120 (1996) 589.